Check for updates

Traffic

WILEY

Traffic

REVIEW OPEN ACCESS

Fluorescent Reporters, Imaging, and Artificial Intelligence Toolkits to Monitor and Quantify Autophagy, Heterophagy, and Lysosomal Trafficking Fluxes

Mikhail Rudinskiy[1,2,3] | Diego Morone[1,2,4] | Maurizio Molinari[1,2,5]

[1]Università della Svizzera italiana, Lugano, Switzerland | [2]Institute for Research in Biomedicine, Bellinzona, Switzerland | [3]Department of Biology, Swiss Federal Institute of Technology, Zurich, Switzerland | [4]Graduate School for Cellular and Biomedical Sciences, University of Bern, Bern, Switzerland | [5]École Polytechnique Fédérale de Lausanne, Lausanne, Switzerland

Correspondence: | Maurizio Molinari (maurizio.molinari@irb.usi.ch)

Received: 30 April 2024 | **Revised:** 21 August 2024 | **Accepted:** 3 October 2024

Funding: This work was supported by Swiss National Science Foundation grants 310030_214903 and 320030-227541, Eurostar E!2228, and Innosuisse 35449.1 IP-LS.

Keywords: artificial intelligence | autophagy | autophagy flux | endolysosomes (EL) | ER-phagy | ER-to-lysosome-associated degradation (ERLAD) | heterophagy | lysosomal storage disorders (LSD) | lysosomes | tandem fluorescent reporters

ABSTRACT

Lysosomal compartments control the clearance of cell-own material (autophagy) or of material that cells endocytose from the external environment (heterophagy) to warrant supply of nutrients, to eliminate macromolecules or parts of organelles present in excess, aged, or containing toxic material. Inherited or sporadic mutations in lysosomal proteins and enzymes may hamper their folding in the endoplasmic reticulum (ER) and their lysosomal transport via the Golgi compartment, resulting in lysosomal dysfunction and storage disorders. Defective cargo delivery to lysosomal compartments is harmful to cells and organs since it causes accumulation of toxic compounds and defective organellar homeostasis. Assessment of resident proteins and cargo fluxes to the lysosomal compartments is crucial for the mechanistic dissection of intracellular transport and catabolic events. It might be combined with high-throughput screenings to identify cellular, chemical, or pharmacological modulators of these events that may find therapeutic use for autophagy-related and lysosomal storage disorders. Here, discuss qualitative, quantitative and chronologic monitoring of autophagic, heterophagic and lysosomal protein trafficking in fixed and live cells, which relies on fluorescent single and tandem reporters used in combination with biochemical, flow cytometry, light and electron microscopy approaches implemented by artificial intelligence-based technology.

1 | Lysosomes and Endolysosomes: A Historical Overview

Russian zoologist Ilja Iljitsch Metchinkoff, awarded with the Nobel Prize in Physiology or Medicine 1908 for the discovery of phagocytosis, was probably the first scientist to observe and report that intracellular digestion proceeds at acidic pH [1]. However, lysosomes, the intracellular organelles storing the hydrolytic enzymes ensuring clearance of macromolecules and portions of other organelles, were isolated [2, 3], named [4, 5] and visualized in light and electron microscopy [6] more than 60 years later. Lysosomes are nowadays considered signaling hubs that modulate protein, lipids, ions, stress and nutrient dynamics [7, 8]. They eventually deliver hydrolases upon fusion with endosomes to generate degradative endolysosomes or with autophagosomes to generate degradative autolysosomes [9–11].

Mikhail Rudinskiy and Diego Morone equally contributed to this work.

This is an open access article under the terms of the Creative Commons Attribution-NonCommercial-NoDerivs License, which permits use and distribution in any medium, provided the original work is properly cited, the use is non-commercial and no modifications or adaptations are made.

© 2024 The Author(s). *Traffic* published by John Wiley & Sons Ltd.

1.1 | The Degradative Compartments Are Acidic Organelles

Endolysosomes stand out due to their physico-chemical properties that govern the biological processes taking place in their lumen. Perhaps the most crucial property of degradative endolysosomes is the acquisition and maintenance of an acidic environment. Although it has been known since the work of Ilya Metchnikoff that lysosomal enzymes require acidic pH to function, the first measurement of lysosomal acidity, with values ranging from pH 4.5–4.8, dates back to 1978 [12]. The low pH of lysosomes and degradative endolysosomes is maintained by Vacuolar (V)-type ATPases that actively pump H^+ ions into the lumen of the organelle. Consistently, cell exposure to the macrolide antibiotic Bafilomycin A1 (BafA1), a selective inhibitor of V-ATPases, neutralizes pH and inactivates the hydrolytic activity of degradative organelles [13–15].

1.2 | Lysosomal Enzyme Trafficking and Lysosomal Storage Disorders

Lysosomal hydrolases are synthesized in the ER. Upon successful completion of the folding program, they enter the secretory pathway, the Golgi compartment and are eventually diverted to the lysosome upon recognition of their N-linked glycans by mannose 6-phosphate receptors (Figure 1, pink arrows). Protein folding is error prone, and missense mutations within the coding sequence of the lysosomal enzymes reduce the ability of the protein to fold and function correctly and are associated with various lysosomal storage disorders (LSDs) [16]. In some cases, the mutation delays conformational maturation, leads to prolonged ER retention, and may result in inappropriate degradation of potentially active proteins (loss-of-function disorders) [17–21]. As a general rule, when mutations do not occur in the enzyme's active site, therapeutic intervention with chemical and/or pharmacological chaperones is an option to protect mutant polypeptides from premature clearance, increase their folding efficiency, stabilize their structure and eventually promote their transport to the intra or extracellular site of activity [22–25]. Crucially, the development and screening of successful therapeutics for LSDs requires quantitative methods to monitor the delivery of hydrolases to the lysosomal compartments.

1.3 | Exogenous or Endogenous Material Cleared Within Acidic Degradative Compartments

Degradative pathways are classified according to the exogenous (*hetero*-phagy) or endogenous (*auto*-phagy) material that they are handling [26, 27].

1.4 | Heterophagy: Lysosomal Clearance of Extracellular Material

Heterophagy consists of uptake and lysosomal degradation of extracellular (i.e., non-self) material [27]. Heterophagy substrates include macromolecules, receptor ligands, pathogens of bacterial, viral or multicellular origin, or cellular debris endocytosed from the extracellular environment (Figure 1). These substrates are engulfed within a portion of plasma membrane that forms an endocytic vesicle [28]. Several endocytic pathways lead to substrate degradation: (i) receptor-mediated endocytosis (also called clathrin-mediated endocytosis): a protein coat basket formed on the inside of the plasma membrane encloses extracellular cargo and fuses with endosomes that eventually merge with lysosomes to degrade the extracellular material; (ii) caveolin-mediated endocytosis: caveolae derived from the plasma membrane fuse with endosomes or lysosomes; (iii) macropinocytosis: macropinosomes engulfing large volumes of extracellular liquids fuse with lysosomes; (iv) phagocytosis: large substrates such as extracellular pathogens or cell debris are engulfed by the cell forming a phagosome, that later fuses with a

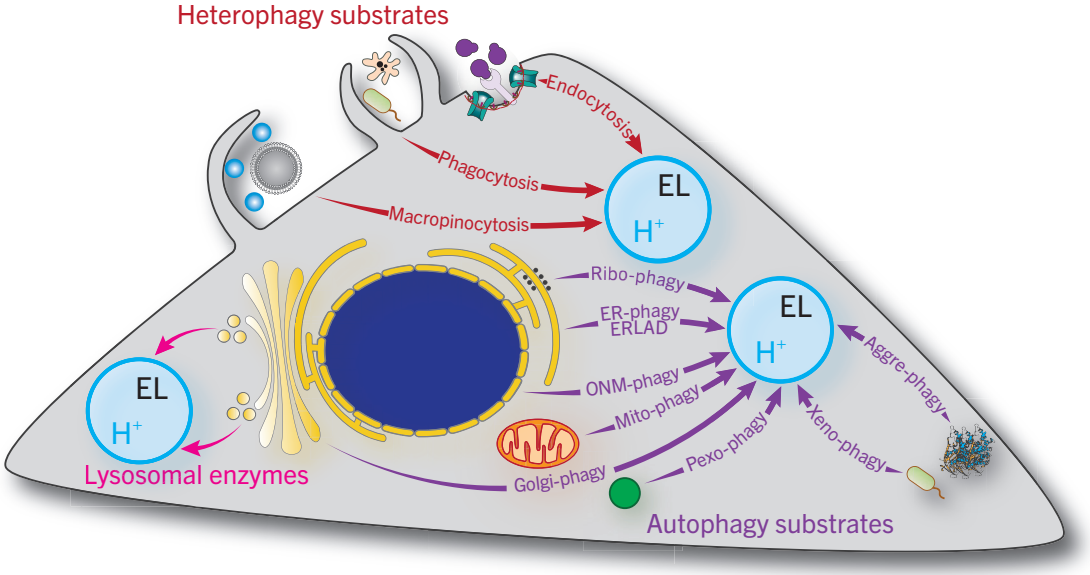

FIGURE 1 | Overview of mammalian lysosomal trafficking pathways. Red arrows indicate hetero-phagy pathways, violet arrows auto-phagy pathways and pink arrows transport of lysosomal enzymes from the site of synthesis (the ER) to their homing organelle, via the Golgi complex. EL, endolysosome; ERLAD, ER-to-lysosome-associated degradation; ONM, outer nuclear membrane.

16000854, 2024, 10, Downloaded from https://onlinelibrary.wiley.com/doi/10.1111/tra.12957 by Biblioteca universitaria di Lugano, Wiley Online Library on [18/11/2024]. See the Terms and Conditions (https://onlinelibrary.wiley.com/terms-and-conditions) on Wiley Online Library for rules of use; OA articles are governed by the applicable Creative Commons License

lysosome (Figure 1, red arrows) [29–34]. Deficiencies within the endocytic pathways are observed in multiple genetic disorders, such as familial pulmonary arterial hypertension [35, 36], lipodystrophy [37], genetic immune disorders [38], cancers [34, 39] and many others.

1.5 | Autophagy: Lysosomal Clearance of Cell-Own Material

Autophagy is the clearance by lysosomal enzymes of cells-own components such as portions of organelles (e.g., mitochondria, the ER, the nuclear envelope, the Golgi, peroxisomes and lysosomes) or of cytoplasmic macromolecules including ribosomes, protein aggregates, glycans and lipid droplets (Figure 1, purple arrows). Autophagic cargo arrives to degradative compartments through a variety of pathways: (i) macro-autophagy involves the formation of double-membrane autophagosomes that capture the material to be degraded and eventually fuse with lysosomes to generate degradative autolysosomes; (ii) micro-autophagy occurs via degradative endolysosomes that directly engulf material to be removed; (iii) LC3-dependent vesicular transport involves fusion of portions of organelles with degradative compartments to release cargo for lysosomal clearance; (iv) chaperone-mediated autophagy relies on receptor-mediated translocation of cytosolic proteins within degradative compartments. The molecular bases of these pathways are thoroughly described in recent reviews [40–50]. Countless diseases are caused by or linked to a deficiency within the autophagic landscape [51–53].

In the context of basic research and drug discovery, the establishment of quantitative methods to monitor the transport of intra- and extracellular material to lysosomal compartments is necessary for the assessment of trafficking and autophagic pathways, to identify and intervene to cure abnormalities that may contribute to pathology. One of the fundamental challenges is the highly acidic and highly hydrolytic environment that rapidly recycles the autophagic clients transported to the degradative organelles. To overcome these restraints researchers developed a toolbox of pharmacological treatments and protein-based reporters to monitor the trafficking of substrates to degradative compartments.

2 | Measuring Substrate Flux to Degradative Endolysosomes

2.1 | Measuring Substrate Flux Upon Lysosomal Inactivation

Material delivered within degradative organelles is rapidly destroyed. Thus, to get information on the magnitude of lysosomal delivery of substrates to be cleared from cells, one option is to inhibit lysosomal hydrolases and quantify the material accumulating within the endolysosomal lumen. To this end, three classical approaches are employed: the first consists in inactivation of lysosomal proteases with a cocktail of cell permeable protease inhibitors. The second exploits the fact that lysosomal hydrolases have an acidic pH-optimum and consists in the pharmacological inhibition of the V-ATPase to neutralize the endolysosomal pH. In the third, compounds such as chloroquine accumulate in the acidic compartment and buffer endolysosomal pH through self-protonation [54]. Although organelles such as Golgi and endosomes have an acidic lumen, they do not reach the acidification level of degradative endolysosomes that ranges between pH 4.5 and 5 [55–58]. Acidification of the endolysosomal lumen favors enzymatic activity of the lysosomal hydrolases and drives conformational changes within substrates thereby priming them to hydrolysis [11, 59]. Inhibitors such as BafA1 or Concanamycin A [13–15] that neutralize endolysosomal pH have been employed by researchers to prevent the degradation and measure the trafficking of endolysosomal cargoes.

Finally, pharmacological inhibition of autophagic flux with chloroquine (or its derivative hydroxychloroquine), is a potent strategy to selectively inhibit autophagosome-mediated delivery of material to-be-degraded. Chloroquine progressively slows down autophagy by preventing lysosome-autophagosome fusion and buffering endolysosomal pH, thus driving the accumulation of cytoplasmic autophagosomes and their cargo [60–64]. Moreover, chloroquine and hydroxychloroquine have been approved by the Food and Drug Administration (FDA) for clinical use and are both widely employed as a chemotherapy against multiple types of cancers, as well as anti-malaria drugs.

Lysosomal inactivators have been extensively used to assess bulk or unspecific autophagic flux. The readout of bulk autophagic flux is based on the measurement of the turnover of ATG8/LC3/GABARAP family member proteins that have entered the degradative pathway (i.e., lipidated at the surface of autophagosomes or endolysosomes) [65–67]. The difference between the amount of lipidated ATG8 proteins present in cells with inhibited autophagic degradation (generally detected in Western Blot as a faster-traveling band compared to the non-lipidated soluble form) and in cells with ongoing degradation indicates the bulk autophagic flux at steady state.

While the protease and lysosomal inactivators have been widely employed to measure autophagic and heterophagic fluxes, it became clear that these pharmacological agents induce indirect effects on cell physiology, such as apoptosis [68], impaired Golgi and endosomal function [64] and increased sequestration of autophagic substrates in autophagosomes or inactivated degradative organelles [69]. Importantly, lysosomal inactivation might enhance LC3/GABARAP lipidation at single membrane endolysosomes [70, 71], directly impacting the quantification of the autophagic flux. Moreover, temporal resolution is often not assessed at all; therefore, the accumulation of the degradative cargo indicates qualitatively, rather than measures quantitatively, the induction of autophagic flux.

2.2 | Measuring Substrate Flux Without Perturbation of Lysosomal Activity

To overcome these pitfalls, researchers developed a long list of protein tags that can be added to autophagy gene products, cargo proteins, lysosomal enzymes to monitor their intracellular trafficking without perturbing the degradative activity or the luminal pH of endolysosomal compartments.

16000854, 2024, 10, Downloaded from https://onlinelibrary.wiley.com/doi/10.1111/tra.12957 by Biblioteca universitaria di Lugano, Wiley Online Library on [18/11/2024]. See the Terms and Conditions (https://onlinelibrary.wiley.com/terms-and-conditions) on Wiley Online Library for rules of use; OA articles are governed by the applicable Creative Commons License

These protein tags exhibit intrinsic fluorescence (e.g., GFP, YFP, RFP, mCherry and Keima), or can bind cell permeable or impermeable fluorescent molecules (e.g., HaloTag [72, 73]). They can be combined in *tandem reporters* (e.g., mCherry-GFP [74, 75] and HaloTag-GFP [76, 77]) to extend their applications and modes of detection (gel electrophoresis, light and electron microscopy, flow cytometry, Figure 2). Their physico-chemical properties, including their stability, may change at the acidic pH of the lysosomal lumen. These lysosomal trafficking fluorescent reporters may be classified into four groups based on their mode of action and the available readouts reporting on their arrival into degradative endolysosomes (see Box 1; Figure 2):

- Tandem Fluorescent Reporters (mTagRFP-mWasabi [78]) (Figure 2A).
- Proteolytic Probes (CCER [79] and HaloTag [77, 80]) (Figure 2B).
- Proteolytic Tandem Fluorescent Reporters (HaloTag-GFP [76, 77, 81] and mCherry/RFP-GFP [74, 75, 82]) (Figure 2C).
- pH-sensitive Fluorescent and Förster/Fluorescence Resonance Energy Transfer (FRET) probes (Keima [83] and Signal-Retaining Autophagy Indicator [SRAI] [84]) (Figure 2D).

The first and so far, most used tandem fluorescent bulk autophagy reporter developed, the mCherry-GFP tag fused at the N-terminus of LC3 [74, 75, 85], fluoresces in GFP and mCherry channels when located outside of acidic degradative organelles. Upon arrival in the acidic environment, the chromophore of acid-sensitive GFP portion undergoes reversible protonation [86, 87], rapidly losing most of its fluorescence. Eventually, GFP β-barrel is destroyed by acids and lysosomal hydrolases [88–90], leading to the irreversible loss of fluorescence. In contrast, acid-insensitive mCherry reversibly loses its fluorescence only at lower pH (pKa of mCherry is below physiologically observed pH levels of 4.5 [86, 91]) and is resistant to the irreversible loss of fluorescence, thus remaining fluorescent upon arrival in the endolysosomal lumen [91]. Therefore, the rate of autophagic flux may be measured by assessing the rate of formation of mCherry-only puncta within LAMP1/RAB7-positive endolysosomes. Following the introduction of mCherry-GFP-LC3, researchers focused on the improvement of signal-to-noise ratio by employing more stable and more acid-sensitive fluorescent proteins (e.g., mTagRFP-mWasabi [78], pHluorin-mKate2-LC3 [92, 93]), adding new modalities to the readouts (e.g., fluorescent in-gel detection of endolysosomal HaloTag fragment [76, 77, 81]), and fluorescent protein multiplexing to differentiate between different stages of autophagy progression [94].

3 | Assessing Cargo-Specific Autophagic Flux

3.1 | Limitations of ATG8-Based Flux Measurements

Flux measurements based on fluorescent tagging of ATG8 family proteins are useful in visualizing the ongoing autophagic activity of the cell. However, they do not report on the

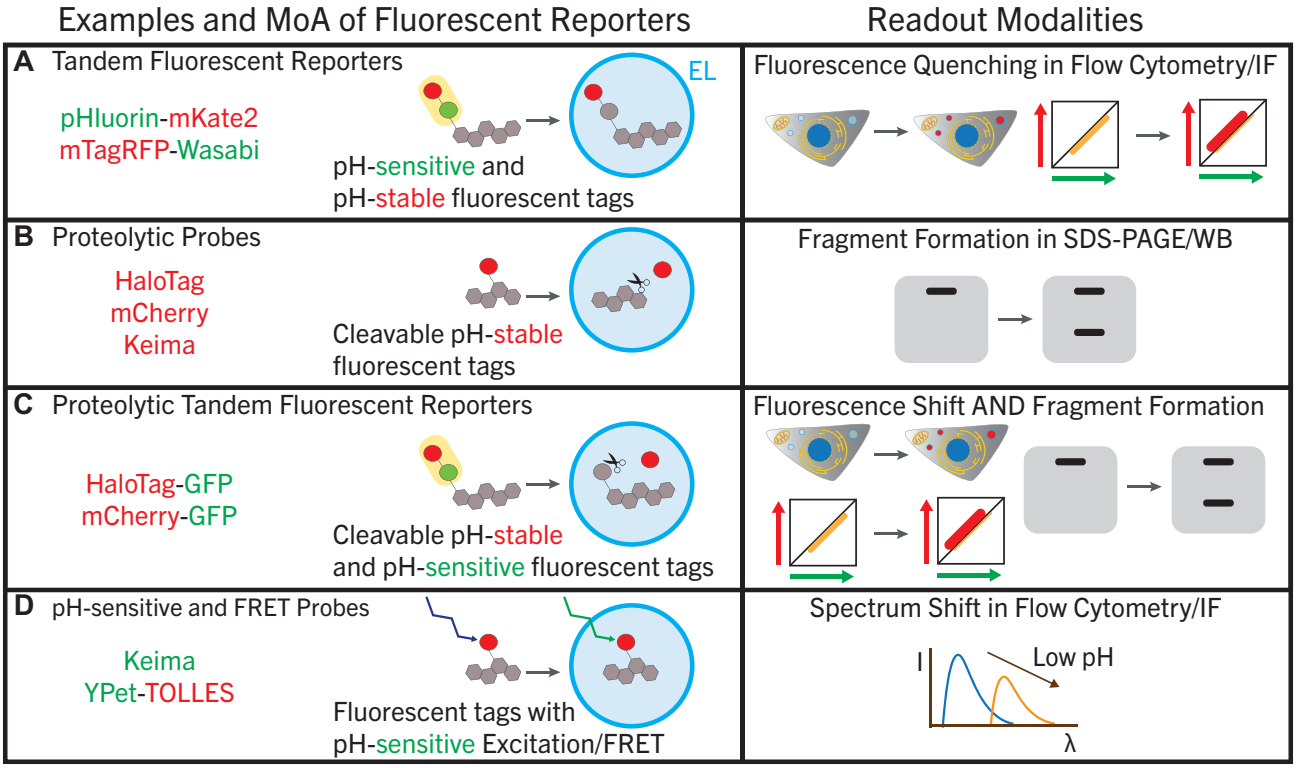

FIGURE 2 | Classes of fluorescent reporters and their read-out modalities for monitoring lysosomal delivery of proteins and organelles. The grouping is decided by the mode of action (MoA) of a reporter and the available readout modalities reporting on lysosomal trafficking. (A) Tandem fluorescent reporters. (B) Proteolytic probes. (C) Proteolytic tandem fluorescent probes. (D) pH-sensitive fluorescent and FRET probes. EL, endolysosome; FRET, Förster/fluorescence resonance energy transfer; IF, immunofluorescence.

16000854, 2024, 10, Downloaded from https://onlinelibrary.wiley.com/doi/10.1111/tra.12957 by Biblioteca universitaria di Lugano, Wiley Online Library on [18/11/2024]. See the Terms and Conditions (https://onlinelibrary.wiley.com/terms-and-conditions) on Wiley Online Library for rules of use; OA articles are governed by the applicable Creative Commons License

BOX 1 | Classes of fluorescent reporters and their use to monitor lysosomal delivery of proteins and organelles.

1. Tandem Fluorescent Reporters

Tandem fluorescent reporters are composed of pH-sensitive and pH-stable portions that change fluorescence emission properties upon delivery to acidic cellular compartments (Figure 2A). Introduction of mCherry/mRFP (acid-insensitive)-GFP (acid-sensitive) tandem fluorescent reporters into the research [74, 75] revolutionized the field of autophagy by allowing precise and live tracking of autophagic events within the cell. These early reporters presented a few weaknesses, related to their sensitivity to acidic environment and overlapping excitation/emission spectra. Reversible loss of GFP fluorescence represents an issue for fixed-sample applications, as the reconstitution of GFP fluorescence upon fixation introduces an error to the measurement, falsely suggesting that a portion of GFP did not enter the acidic environment. This limitation [75] has been solved by substituting GFP moiety with mWasabi [78] and later with pHluorin [92, 93] that demonstrated higher pH sensitivity of the reporter due to higher pKa of GFP variants [95], and higher proportion of irreversible to reversible fluorescence. Similarly, the development of RFP/mCherry variants with lower pKa values and high resistance to lysosomal proteases would result in more acid-stable emission.

Another issue with early tandem-fluorescent reporters is the overlap between GFP's emission spectrum and the excitation spectrum of RFP/mCherry, leading to the formation of an unwanted, low efficiency, FRET pair. The loss of the mCherry signal inside acidic organelles due to the reduction in FRET between the two parts of the reporter introduces another variable into the quantification of the signal. This shortcoming has been addressed by utilizing acid-sensitive/acid-insensitive fluorophore pairs with smaller spectral overlap (e.g., by substituting mCherry with mKate2 [92, 96]) that allowed monitoring of autophagy events in far red range thus reducing phototoxic effects during live measurements. Since their introduction, tandem fluorescent reporters have been extensively used to monitor bulk and cargo-specific autophagy fluxes, as well as trafficking of endocytosed plasma membrane proteins to endolysosomes [97, 98].

2. Proteolytic Probes

Proteolytic autophagic probes rely on the activity of acidic lysosomal hydrolases that cleave a portion of a reporter, thus creating a stable reporter fragment that can be detected by gel electrophoresis or by Western Blot (Figure 2C). These reporters generally consist of a stable detectable portion (fragment) and a cleavable linker sensitive to lysosomal proteases. For organellophagy applications, cleavable linkers are often not necessary as the cargo proteins themselves are processed or degraded within the lumen of the lysosomes [99]. In mammalian cells, HaloTag [76, 77], Keima [100] and RFP/mCherry [79] fusion proteins are used as autophagy flux reporters, as they produce a Western blot-detectable fragment upon processing by endolysosomal enzymes. HaloTag is an inactive bacterial dehalogenase containing a pocket designed to covalently bind cell-permeable chloro- and bromo-alkanes that can be modified with synthetic fluorescent probes [72]. HaloTag fragment labeled with a fluorescent ligand retains its fluorescence when separated by gel electrophoresis, and thus is detectable by laser scanning of the electrophoretic gel [76, 77, 81]. The fluorescent HaloTag pulse-chase technique, consisting of sequential labeling of HaloTag-fusion proteins with fluorescent and nonfluorescent ligands, allows precise measurement of degradation kinetics of different substrates [73, 76, 101].

3. Proteolytic Tandem Fluorescent Reporters

Autophagy flux reporters combining the properties of tandem-fluorescent and proteolytic probes allow multiple readouts, and thus are used to characterize autophagy pathways by multiple methods. RFP-GFP reporter undergoes proteolytic cleavage in the acidic environment of the endolysosome, producing a RFP fragment, which is detectable by immunoblotting [82]. More advanced tandem fluorescent proteolytic HaloTag-GFP reporter allows the monitoring of bulk [77] and cargo-specific [76] autophagic events by light microscopy (by observing the accumulation of HaloTag-positive/GFP-negative puncta within acidic endolysosomes), by flow cytometry (measuring the quenching of GFP fluorescence) and by measuring the amount of HaloTag fragment by sodium dodecyl-sulfate polyacrylamide gel electrophoresis (SDS-PAGE), as well as degradation kinetics measurements [101] (Figure 2B). Finally, fragments of other pH-stable fluorogenic proteins might theoretically be observed by immunoblotting, suggesting that tandem-fluorescent reporters such as pHluorin-mKate2 and mTagRFP-Wasabi (Figure 2A) might, in theory, be used as proteolytic tandem-fluorescent reporters.

4. pH-sensitive Fluorescent and FRET Probes

Earlier issues with false positive readouts based on GFP fluorescence inside acidic lysosomes, as well as a larger size of tandem-fluorescent reporters suggested the need for the development of a complementary system to report on autophagy events. The observation that the pH sensitive protein Keima changes its excitation wavelength in the acidic environment of the degradative endolysosomes (Figure 2C) led to its use in monitoring non-selective (bulk) autophagy events [102], cytosolic turnover [103], mitophagy (by adding a mitochondrial signal sequence at the N-terminus of the protein [83, 104, 105]), pexophagy [106] and ribophagy [100, 107]. Despite the reliable results, Keima reporter is prone to a permanent excitation wavelength shift upon prolonged light exposure, reverts its wavelength shift during cell fixation protocols making it suitable exclusively for live imaging applications, and its use requires a technically complex dual-excitation imaging system [108].

To address these issues, a complementary system based on FRET was introduced. The SRAI reporter [84] is composed of an extremely acid-resistant cyan-emitting fluorescent protein (afCFP) derived from Anthozoa coral [109] (thus named TOLLES, TOLerance of Lysosomal EnvironmentS), and an acid-sensitive yellow fluorescent protein YPet. The YPet (acceptor)–TOLLES (donor) pair is a potent FRET tandem, functioning exclusively outside the acidic compartment [110]. Outside of degradative organelles, mainly YPet fluorescence is observed, while upon the degradation of YPet inside degradative organelles, TOLLES fluorescence is predominant as it is not absorbed anymore by the acceptor [110]. Contrary to mCherry/RFP-GFP reporters, that exhibit residual unwanted FRET activity that is difficult to account for, the readout of YPet-TOLLES reporter is highly quantitative and

16000854, 2024, 10, Downloaded from https://onlinelibrary.wiley.com/doi/10.1111/tra.12957 by Biblioteca universitaria di Lugano, Wiley Online Library on [18/11/2024]. See the Terms and Conditions (https://onlinelibrary.wiley.com/terms-and-conditions) on Wiley Online Library for rules of use; OA articles are governed by the applicable Creative Commons License

BOX 1 (Continued)

specific to the acidic environment of the endolysosomes. Such FRET readout allows monitoring of bulk [111], ER [111] and mitochondrial [84] autophagy fluxes in living cells and tissues, as well as in fixed samples, and has a potential to become a go-to tool for researchers performing autophagy flux measurements.

rate of delivery of specific cargoes, and they are not suitable for monitoring non-autophagic trafficking of endocytosed substrates and lysosomal hydrolases, nor the autophagic trafficking independent of ATG8 proteins [112, 113]. Moreover, levels of lipidated ATG8 proteins are subject to intrinsic variation due to the presence of multiple adaptor proteins with varying degradation rates (LC3 proteins vs. GABARAPs) [114], high background signal due to ongoing bulk autophagy in cells at steady state [115] and incorporation into intracellular aggregates [116, 117]. Furthermore, the level of LC3 lipidation does not necessarily reflect ongoing autophagy as it may be induced indirectly, for example, by chemical treatments preventing autophagic flux [70].

Autophagy adaptor proteins (e.g., p62/SQSTRM1) and autophagy receptors fused to a fluorescent flux reporter are used as reporters of selective autophagic flux within a specific pathway [75, 118]. However, they often do not reflect the real degradation rate of the substrate protein or the organelle, as they are more efficiently removed than their cargo due to a direct interaction with ATG8 family proteins [115]. Moreover, overexpression of reporter-tagged receptors results in an upregulation of autophagy and an increase in autophagic flux [76, 119–122]. Therefore, endogenous tagging of ATG8-interacting proteins is often required to analyze the effects of autophagy-inducing stimuli.

3.2 | Fluorescent Reporters to Study Organellophagy and Xenophagy

Organellophagy, that is, the fragmentation and lysosomal delivery of mitochondria, ER, Golgi and other organelles for clearance has first been observed more than 70 years ago (for mitophagy [27, 123–126], ER-phagy [27, 127–133]). Despite early observations, quantifying degradation rates of specific organelles, such as mitochondria and ER by cargo degradation assays has been historically challenging due to small relative changes in organelle-specific protein abundance levels induced by autophagy cues. Amino acid starvation (a strong physiological autophagy cue) causes clearance of 7.8% of ER protein content [134] (after 10 h) that can hardly be assessed only with complex quantitative proteomics assays [134, 135]. Similarly, mitophagy induction by starvation or hypoxia is not observable by conventional biochemical measurements of mitochondrial protein abundance changes within the cell [136].

Monitoring the delivery of organelle portions to lysosomes provides a simple way of measuring organelle delivery to degradative endolysosomes. First quantitative measurement of organelle autophagy flux in mammalian cells were performed by attaching the pH-sensitive and protease-resistant protein Keima to the mitochondrial signal sequence (mt-Keima) [83]. Keima is an engineered 31 kDa fluorescent protein derived from stony coral *Montipora* [137]. The chromophore of Keima is present in either neutral or ionized state, depending on the pH of the environment, resulting in two distinct excitation peaks corresponding to the neutral and ionized states of the phenolic hydroxyl moiety of the chromophore. Upon arriving within acidic degradative endolysosomes, the reversible shift in the excitation wavelength allows precise monitoring and quantification of autophagic events in live imaging setups [83, 103, 136, 138, 139].

The direct measure of the delivery of organelle components to degradative organelles reduces the measurement error present when using bulk autophagic flux as a readout and is generally pathway-agnostic. Therefore, the use of Keima tag has been further expanded beyond mitophagy applications to monitor ER-phagy [134, 135], ribophagy [100, 107] and Golgiphagy [140] (Figure 1). As the quantitative organelle flux measurements have been established for Keima, other fluorescent reporters have been used for the assessment of the magnitude of organelle-specific autophagy. This trend is clearly illustrated by the multitude of ER-phagy substrates monitored with fluorescent reporters. Lysosomal ER turnover has been dissected using luminal tandem fluorescent ssRFP-GFP-KDEL [134] and ER membrane mCherry-RAMP4 (CCER [79]), Keima-RAMP4 [135] and tandem-fluorescent GFP-mCherry-RAMP4 (EATR [79, 141, 142]), as well as ER compartment-specific ER sheets (CLIMP63-mCherry-GFP [141]) and ER tubules (REEP5-mCherry-GFP [135, 141]) fluorescent reporters (see Box 1). Furthermore, the kinetics of autophagic clearance of ER portions containing ER-phagy receptor SEC62 [143, 144] or containing misfolded proteins [145, 146] were measured by HaloTag-GFP reporter [76, 145–148].

Similarly, xenophagy (foreign-eating), a process of elimination of intracellular pathogens by degradative endolysosomes, may be theoretically explored and quantified with fluorescent reporters. So far, the visualization of pathogens inside endolysosomes is restricted to light [149, 150] and electron microscopy micrographs of cells, but the quantitative assessment of these events with fluorescent reporters is conceivable.

3.3 | Fluorescent Reporters to Study ERLAD

The misfolded polypeptides produced in the ER are cleared via ER-associated degradation (ERAD) or via ER-to-lysosome-associated degradation (ERLAD). ERAD proceeds upon translocation of the misfolded protein across the ER membrane into the cytosol, where it is poly-ubiquitylated and degraded by 26S proteasomes. ERLAD intervenes to remove

16000854, 2024, 10, Downloaded from https://onlinelibrary.wiley.com/doi/10.1111/tra.12957 by Biblioteca universitaria di Lugano, Wiley Online Library on [18/11/2024]. See the Terms and Conditions (https://onlinelibrary.wiley.com/terms-and-conditions) on Wiley Online Library for rules of use; OA articles are governed by the applicable Creative Commons License

ER portions that contain misfolded polypeptides that fail to be translocated across the ER membrane and to enter ERAD pathways [101, 145, 151].

ERLAD is responsible for disposal of a variety of misfolded substrates [152]. The paradigmatic example of an ERLAD client is ATZ, the Z variant of α1-antitrypsin featuring an E342K point mutation within its polypeptide sequence that significantly amplifies its propensity for polymerization [153–157]. The polymers of ATZ are too large to enter ERAD pathways and are instead segregated in ER subdomains that are eventually delivered to endolysosomes for clearance [101, 146, 153, 154, 158–160]. Fluorescent reporters have been employed to monitor the trafficking of ATZ polymers to degradative endolysosomes: pulse-chasable proteolytic HaloTag probe was used to measure the degradation kinetics of ATZ [101], while the proteolytic tandem fluorescent HaloTag-GFP reporter was employed to measure the time course of delivery of ATZ to degradative compartments [76]. Other ER-localized misfolded polypeptides, whose ERLAD has been dissected with fluorescent reporters include misfolded procollagen [161, 162] and P3H4 [163].

3.4 | Fluorescent Reporters to Study Heterophagy

Selective and non-selective endocytic pathways converge on the endolysosome for degradation of extracellular and plasma membrane components (Figure 1). Tandem-fluorescent reporters have been employed to monitor heterophagic events, such as during endocytosis of extracellular misfolded proteins (e.g., amyloid precursor protein [97], alpha 2-macroglobulin [164] and heat-misfolded Clusterin [165] as well as during the regulation of glucose signaling through GLUT1 glucose transporter endocytosis [98]). However, the adoption of these techniques is significantly lagging in the fields of heterophagy. Fluorescent reporters have a potential to fast-forward drug discovery for diseases associated with these pathways that include neurodegenerative disorders, cancer and immune disorders.

4 | Monitoring Lysosomal Delivery of Hydrolases for Pharmacologic Intervention in LSDs

Owing to the pathway-agnostic mode of action of cargo-specific fluorescent reporters, they may be repurposed to monitor the delivery of lysosomal-resident proteins to their homing organelle. Lysosomal enzymes are synthesized in the ER and are transported to their site of activity through the conventional secretory pathway. Several LSDs are caused by genetic missense mutations affecting the tertiary structure of lysosomal enzymes and preventing their trafficking to the degradative organelles. For example, mutations that impair conformational maturation of β-glucocerebrosidase, galactocerebrosidase, or α-galactosidase cause Gaucher [166], Krabbe [167, 168] and Fabry [169, 170] diseases, respectively.

The application of autophagy reporters to monitor the delivery of lysosomal enzymes is still very limited. We have recently demonstrated the practicality of fluorescent reporters in assessing the efficiency of lysosomal trafficking of disease-relevant mutant polypeptides by employing the proteolytic HaloTag probe in cellular models of GM1-gangliosidosis and Morquio B disease [80]. These rare and phenotypically distinct genetic disorders are caused by destabilizing missense mutations within the lysosomal β-galactosidase enzyme [17, 171–173]. The amount of HaloTag fragment formed upon the arrival of mutant polypeptides within acidic endolysosomes was significantly reduced because of missense amino acid substitutions affecting the folding of the enzyme within the ER (Figure 2B). Enhancement of HaloTag fragment production was a simple read-out to assess the capacity of allosteric pharmacological chaperones to enhance the trafficking of the mutant hydrolases, and reduce the accumulation of toxic GM1 ganglioside substrate, serving as proof-of-concept that fluorescent reporters may (and should) be exploited within the drug discovery pipelines for the screening and identification of therapeutic compounds [80]. Inducible mCherry-GFP reporter was used to monitor the delivery of lysosomal DNASE2 in a time-resolved manner [174, 175].

5 | In Vivo Applications of Cargo-Specific Autophagy and Lysosomal Transport Reporters

In vivo monitoring of the degradation of disease-relevant substrates, such as damaged mitochondria or misfolded ER proteins and delivery of lysosomal enzymes, represents a concrete application of cargo-specific autophagy and lysosomal transport reporters [80, 115, 152, 176, 177]. Due to the high specificity of the readout, employing cargo-specific autophagy flux reporters would allow identification and pre-clinical testing of target-specific modulators of autophagic degradation and protein trafficking [80, 141, 178].

Several autophagy and lysosomal transport reporters are suitable for animal model applications. For these purposes, the use of reporters with robust expression in the tissue of interest and minimal side effects is essential. Transgenic mice expressing the mCherry-GFP reporter targeted to outer mitochondrial membrane (mito-QC) demonstrated that extensive mitophagy is taking place in multiple organs during development and in adult mice [179, 180]. Similarly, mice expressing pHluorin-LC3-mCherry were employed to dissect autophagic responses to nutrient deprivation in different organs and to monitor the crosstalk between autophagy and insulin secretion [181]. SRAI reporter is particularly well suited for in vivo applications due to low phototoxicity during imaging, and highly quantitative readout in live imaging and fixed tissues. Adeno-associated virus delivery of Mito-SRAI was used to measure toxin-induced mitophagy responses in non-dopaminergic neurons in a mouse model of Parkinson's disease [84]. Mice expressing the mRFP-GFP-KDEL ER-phagy reporter demonstrated the active role of ER-phagy receptor FAM134C in mediating nutrient deprivation responses in mouse liver [182]. Finally, mt-Keima transgenic mice allowed the characterization of a wide range of physiological and disease-related mitophagy responses [138]. As the availability of in vivo-suitable autophagy reporters grows, we expect to see the implementation of these and other novel animal reporter models in the drug discovery pipelines.

16000854, 2024, 10, Downloaded from https://onlinelibrary.wiley.com/doi/10.1111/tra.12957 by Biblioteca universitaria di Lugano, Wiley Online Library on [18/11/2024]. See the Terms and Conditions (https://onlinelibrary.wiley.com/terms-and-conditions) on Wiley Online Library for rules of use; OA articles are governed by the applicable Creative Commons License

6 | Microscopy Techniques for Monitoring Proteins and Organelles Delivery to Degradative Endolysosomes

6.1 | Light Microscopy Techniques for Visualizing Autophagy Flux and Lysosomal Delivery

In the last decades, light microscopy proved to be one of the major techniques to monitor intracellular events in space and time. Since the 1960s, the parallel advancements of fluorescent probes and light microscopy techniques, especially confocal, have been instrumental to most of biological applications for their combined ability in highlighting—at high resolution—structures of interest from background [183] (Figure 3A). Still, technical limitations do not currently allow us to "visualize everything, everywhere and at the same time" [184].

Thus, the choice of light microscopy technique can be globally trimmed down to the choice between a different combination of three parameters: speed, resolution and photodamage.

6.1.1 | Fixed Cell Light Microscopy

Low-speed, high-resolution, high-power techniques such as laser-scanning confocal microscopy are ideal for the investigation of fixed samples. Confocal microscopy's ability to remove signal from out-of-focus planes together with double- or triple-labeling experiments enables a precise three-dimensional

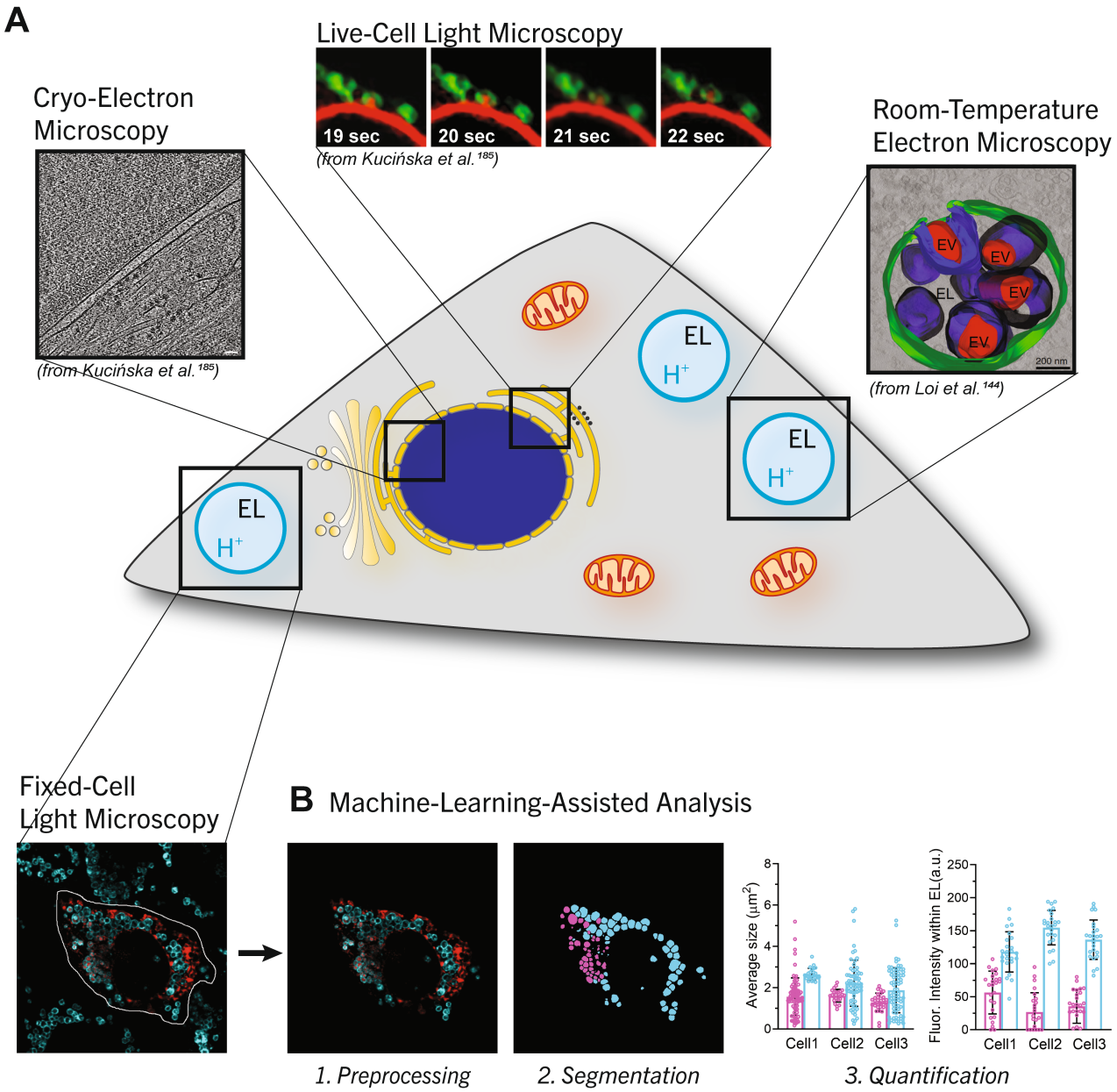

FIGURE 3 | Overview of image acquisition and analysis methods. (A) Light and electron microscopy methods for visualizing protein and organelle flux to lysosomes. Cryo-EM and selected frames of a Live-Cell Light Microscopy movie were adapted from Kucińska et al. [185] (CC-BY 4.0), the RT-EM micrograph is adapted from Loi et al. [144] (CC BY-4.0). (B) Example of a machine-learning pipeline applied to light microscopy images, illustrating the steps for machine learning-assisted image analysis. a.u., arbitrary unit; EL, endolysosome; EV, ER-derived vesicles.

16000854, 2024, 10, Downloaded from https://onlinelibrary.wiley.com/doi/10.1111/tra.12957 by Biblioteca universitaria di Lugano, Wiley Online Library on [18/11/2024]. See the Terms and Conditions (https://onlinelibrary.wiley.com/terms-and-conditions) on Wiley Online Library for rules of use; OA articles are governed by the applicable Creative Commons License

localization of the proteins or organelles of interest. Monitoring the fluorescence reporters that we mentioned in the first part by confocal microscopy [186] provides the ability to precisely discriminate the spatial localization of substrates relative to the degradative organelle (i.e., inside the degradative organelle vs. close to its membrane) [101]. Furthermore, the development of non-fluorescent reporters that can covalently bind to an exogenous fluorophore ligand (such as HaloTag [72, 187], Snap-Tag [188, 189] and Clip-Tag [190]) allowed the visualization of autophagic events with pulse-chase experiments, thus combining high spatial resolution with temporal information [76, 77, 147]. Of note, fixation and permeabilization of the sample can introduce chemical modifications that might potentially alter fluorescence intensity and affecting quantification. Some reporters (e.g., Keima-based) are affected by the environmental pH, and may change their fluorescent properties during cell's preparations for microscopic analyses, thus becoming unsuitable for imaging of endolysosomal trafficking in fixed samples [83]. Other fluorophores (e.g., mCherry) can lose their fluorescence if the fixation/permeabilization protocol does not maintain the pH of the subcellular compartment where the reporter is located. All in all, we consider that reporters based on ligand fluorescence (e.g., HaloTag-based) and FRET probes (e.g., SRAI) that are not affected by changes of the pH during sample processing are better suited for use in fixed samples.

Still, low-speed, high-resolution confocal microscopy falls short when trying to increase the number of conditions or measurements (such as in high-content screenings) or when trying to assess small structures in greater detail. On one hand, techniques such as spinning-disk confocal microscopy can improve the acquisition speed of 3D volumes [186, 191], thus increasing the sample throughput when analyzing fluorescence localization and overlap in complex screenings involving a 3D morphology [192, 193]. On the other hand, confocal microscopy's resolution is limited by light diffraction, effectively limiting the minimum size of resolved structures to a few hundred nanometers. This constraint limits the ability to quantify and morphologically characterize smaller structures such as intra-lysosomal vesicles, protein clusters or organelle fragments.

The advent of super-resolution techniques transformed the physical limit of light diffraction into a technical limit [194, 195]. Super-resolution techniques break light's diffraction limit by using a common principle, with different implementations: one can precisely determine the position of a fluorescent molecule, even if its emission spot is still diffraction-limited and thus much bigger than the molecule itself, if the fluorescence molecule can be turned on or off at different times or at different locations [196]. This principle can take two different implementations: on one hand, localization super-resolution techniques, such as STORM, PALM and their derivatives [197], achieve the increase in resolution by stochastic activation or blinking (*on/off at different times*) of photoconvertible, photoactivable, or blinking dyes while recording many subsequent images of a single field of view. The number of images needed to achieve a sufficient confidence in localization obviously depends on the amount of signal and the specific technique used, but it is usually in the order of the thousands. On the other hand, scanning super-resolution techniques, such as Stimulation Emission Depletion (STED) [198] and its derivatives RESOLFT (Reversible Saturable OpticaL Fluorescence Transitions) [199], MINFLUX [200, 201] and MINSTED [202, 203], achieve the goal by sequentially turning on/off portions of the sample with laser scanning (*on/off at different positions*). All these techniques are beginning to enter the fields of lysosomal trafficking and autophagy, with some notable applications including the use of localization microscopy to study of ULK1 oligomerization and initiation of autophagy [204, 205].

Lastly, expansion microscopy aims at achieving super-resolution by isotropically increasing the sample size and taking advantage of conventional, diffraction-limited, microscopy. In this case, a fixed sample is embedded in a gel, which is then expanded with water [206]. This technique retains endogenous fluorescence and is compatible with standard immunofluorescence protocols. It has been instrumental for the visualization, through confocal and in great detail, of LAMP1 and LC3 localizations [207].

6.1.2 | Live Cell Light Microscopy

In live cell imaging experiments, an event-of-interest is followed by consecutive recording of images to form a so-called time-lapse movie (or time series) [208]. Confocal microscopy, either in single point scanning version or spinning disk confocal microscopy [191], is also well-suited for live cell imaging experiments (Figure 3A, Live-Cell Microscopy inset). For example, spinning disk has been applied to define the role of p62, NBR1 and TAX1BP1 in ubiquitin condensate formation [118], or to monitor the translocation of ATG13 during starvation and drug-induced mitophagy [209]. Live confocal point-scanning microscopy has been used to visualize the endosomal engulfment of outer nuclear membrane portions [185]. Nonetheless, the high-power lasers needed by these techniques limit the acquisition of live events to short times, due to the increased damage of fluorophores (photobleaching) or the activation of light-induced death pathways (phototoxicity), collectively defined as “photodamage.” Longer time series are obtained with more gentle techniques such as widefield live-cell imaging [210], total internal reflection microscopy (TIRF) as in the case of visualization of lysosome fusion with plasma membrane [211], or lattice light sheet microscopy [212, 213].

Super-resolution techniques have also been applied to live cell imaging, with the first applications being with a technique called Structured Illumination Microscopy (SIM) [208, 214]. This technique takes consecutive widefield images of the same field of view with different illumination beam structures to increase the amount of information. The information is then processed to improve the image's resolution [215–217]. Given that SIM is essentially a widefield technique, it is particularly well applicable to live cell imaging although it does not provide the same resolution as the two super-resolution techniques described above. Of the latter two, scanning techniques have inherently been more suitable for live cell imaging, due to the immediacy of their scanning compared to the many images needed for localization microscopy to determine fluorophore location with sufficient accuracy. In their first iterations, scanning super-resolution techniques have been suffering from the same limitations as confocal microscopy, namely photodamage. Nonetheless, they have also been applied to short live cell imaging, as in the imaging of lysosomal fusion-fission processes [218]. Recent developments

16000854, 2024, 10, Downloaded from https://onlinelibrary.wiley.com/doi/10.1111/tra.12957 by Biblioteca universitaria di Lugano, Wiley Online Library on [18/11/2024]. See the Terms and Conditions (https://onlinelibrary.wiley.com/terms-and-conditions) on Wiley Online Library for rules of use; OA articles are governed by the applicable Creative Commons License

(namely MINFLUX and MINSTED) allowed for a dramatic decrease in light power, while retaining good contrast and up to nanometer-level resolution [203, 219]. This makes it possible the application of STED in live cells to the measure mitophagy with mt-Keima [139].

Finally, we should mention that fluorescent reporters offer more information than revealing the localization of the chimeric polypeptides or its abundance. Properties such as fluorescence fluctuations, polarization, or emission decay inform on the dynamics of interaction of the reporter with other proteins or with the microenvironment. For example, the quantification of fluorescence emission decay (lifetime) at each imaging point is used in Fluorescence Lifetime Imaging (FLIM) to determine a lifetime map, which is concentration-independent but microenvironment-dependent and may inform on local pH, ion, or metabolite concentrations, at confocal resolution, or even at super-resolution [220, 221]. In combination with FRET sensors, FLIM-FRET also allows a precise quantification of events such as protein–protein interactions in live cells and at short range (up to 10 nm). Notably, FLIM-FRET has been used to monitor the modes of action of ATG4B during autophagy and the priming of LC3B by ATG4B through the use of a pH-resistant FRET pair [222], or for the investigation of multiprotein interactions in the mTORC1 pathway [223]. FLIM-FRET has also been instrumental for the characterization of competitive inhibition of phosphatic acid with ATG3-ATG8e and ATG6-VPS34 [224], and to highlight the role of VAMP7 hetero-trimerization with Syntaxin-17 and SNAP29 the stability of the SNARE complex upon autophagosome formation [225].

In summary, the high contrast and subcellular resolution of light microscopy, both in its established techniques and latest developments, provide many advantages to investigate the dynamic aspects of autophagy and lysosomal transport. Particularly, the techniques relying on change in local microenvironment (such as FLIM and FLIM-FRET) are a promising tool for the investigation of trafficking events to highly acidic degradative organelles.

6.2 | Electron Microscopy Techniques in Autophagy Research

Electron microscopy (EM) has been crucial in studying autophagy pathways since its introduction into the biological research in the 1950s [226]. Long before the advent of genetic manipulation in the 1990s, which made possible the determination of the autophagy genes in yeast, transmission EM (TEM) revealed the first images of autophagosomes [227]. TEM was also instrumental to the characterization of other types of autophagy, such as mitophagy [227], rough ER autophagy [123], pexophagy [125, 228], and for the detailed description of endocytic events [229], and of lipid droplets engulfment in autophagosomes [230]. Nowadays, EM techniques are used to study the morphology of autophagic structures, helping in identifying their content and supporting other quantitative techniques.

6.2.1 | Room Temperature Electron Microscopy

Common TEM techniques for exploring autophagy in cell cultures employ room temperature chemical fixation, lipid staining with contrast agents based on heavy metals, resin embedding and cutting in ultrathin (~100 nm) sections [231]. A certain degree of 3D information can be obtained by acquiring EM images at different sample tilt angles and performing tomographic reconstructions (electron tomography or ET in short) [232] (Figure 3A, Room-Temperature Electron Microscopy inset). The presence of specific markers on the structure of interest can be assessed by immunostaining with target-specific primary antibodies and colloidal gold particles (usually a few nanometers in size) attached to secondary antibodies. A subsequent gold enhancement step amplifies the contrast of these particles [233, 234]. For example, this technique proved useful for the visualization of ultrastructures marked with endogenous LC3B [235] or to ascribe to micro-ER-phagy the catabolic pathways operating in mammalian cells during recovery from ER stress [143, 144]. Finally, volume EM is a group of techniques, based on transmission (TEM) or scanning electron microscopy (SEM) that reveals 3D structures across depths of the order of the micrometer or more [236, 237]. A low-throughput approach to volume EM can be obtained with manual cutting of sequential slices for acquisition and registration to a final volume, but this limits the amount of volume that can be reconstructed. More sophisticated approaches use automatic cutting and acquisition as in serial block face SEM, or sample ablation with a focused ion beam to expose a new portion for FIB-SEM milling. The latter technique has been used to reconstruct the engulfment of ER exit sites (ERES) by the autolysosome [238].

6.2.2 | Correlative Light-Electron Microscopy

Electron microscopy images, while providing amazing structural information, are sometimes difficult to interpret [239]. The combined use of light and electron microscopy on the same sample (CLEM for Correlative Light-Electron Microscopy) can overcome this limitation, taking advantage of nanometer resolution of EM and multichannel protein localization of lysosomal and cargo markers of light microscopy. A major limitation of the "correlative" part of CLEM is the difference in resolution between light and electron microscopy, which can make it difficult to spot in the EM micrographs the correct organelle that provided fluorescence emission. A second limitation is the compatibility in sample preparation between the two techniques [240]. Differences in solutions used to prepare the samples for light and for EM analyses can result in sub-optimal fluorescence emission, in loss of ultra-structural information (e.g., loss of organellar membranes), or can result in high autofluorescence levels during EM sample preparation. Finally, a third limitation comes from the difference in throughput between the two techniques: while in light microscopy one can easily acquire 3D reconstruction of whole cells, electron microscopy visualizes much smaller volumes and the analysis is often limited to one or few ultrathin slices. As such, finding the right compromise between high resolution, sample processing speed and amount of multichannel information can often be quite time consuming.

6.2.3 | Cryo-Electron Microscopy

While room-temperature electron microscopy techniques provide excellent nanometric resolution and have been established

16000854, 2024, 10, Downloaded from https://onlinelibrary.wiley.com/doi/10.1111/tra.12957 by Biblioteca universitaria di Lugano, Wiley Online Library on [18/11/2024]. See the Terms and Conditions (https://onlinelibrary.wiley.com/terms-and-conditions) on Wiley Online Library for rules of use; OA articles are governed by the applicable Creative Commons License

over the last few decades, a higher resolution might be desirable to resolve finer structures, such as the structures of protein clusters, the contact site between organelles or the distance between two membranes (Figure 3A, Cryo-Electron Microscopy inset). Achieving higher, sub-nanometric, resolution requires changes both in sample preparation and in image acquisition pipeline, with the key element in both cases being the use of very low temperatures. One of the major limitations in sample preparation is the slow speed of chemical fixation when compared to cryo-fixation, due to diffusion of fixative and limiting cross-linking times. In this respect, a faster fixation can be achieved by freezing the sample with mixtures of ethane or ethane/propane at very low temperatures (cryo-fixation) to prevent the formation of ice crystals that would disrupt the cell structure [241, 242]. Notably, cryo- fixation is performed without toxic chemical agents that might introduce artifacts per se. From the acquisition side, these very low temperatures provide another key advantage when pursuing sub-nanometric resolutions: the colder the sample, the less the atomic movement. Latest technical implementations provide an atomic resolution [243–245], and have been instrumental for example to establish the architecture and dynamics of the PI3KC3 complex containing ATG14 [246]. Even at lower resolutions, the use of cryo-EM in its current variations (cryo-TEM, and in particular cryo-ET and the latest cryo-FIB that combines imaging with a focused ion beam that burns the outer layer of biological samples to achieve automated reconstructions of thicker sections [247, 248]) has been instrumental for in situ structural analysis of shape transitions during autophagosome formation [249] and for the elucidation of the mechanisms of nuclear envelope swelling during stress and subsequent lysosomal degradation of excess outer nuclear membrane [185].

6.2.4 | Correlative Cryo-Electron Tomography

Correlative microscopy in cryo conditions is an emerging technology with great potential, due to the preservation of structural details, very high resolution and capacity to retain fluorescent signals [250]. An example is the use of correlative cryo-ET to resolve the different steps of autophagosome biogenesis in yeast [249]. This technique has been applied to the reconstruction of tubular ER portions within the autophagosome in neuronal projections [135, 251].

All in all, electron microscopy has and still is contributing to providing ultrastructural 2D and 3D information, as well as informing on the localization of selected proteins. Incidentally, both light microscopy and room-temperature EM benefited from the protocols developed for cryo-EM. Freeze substitution techniques can bring a cryo-fixed sample to room temperature while preserving its structure. This proved useful both in the preservation of structures that might be altered (in some cases, severely altered) by chemical fixation for use in light microscopy or room-temperature EM [207, 252–255].

7 | Quantitative Assessment of Microscopy Images and Its Automation

Quantification of imaging data relies on well-conducted, unbiased image analyses. Automating image analysis through sets of reproducible protocols plays a key role, along with good practices of data and image acquisition reporting [256]. A standard image analysis workflow involves a preprocessing phase, followed by segmentation and feature quantification (Figure 3B).

Preprocessing steps aim at reducing potential artefacts and improving the contrast or resolution. The reduction of potential artefacts is achieved by different techniques: denoising algorithms reduce image noise, thus improving signal-to-noise ratio [257]; registration algorithms help in aligning images when the acquisition cannot be performed in stable conditions, such as in the case of in vivo imaging [258–260] or when aligning images from different modalities, such as in CLEM. Registration is also currently used in EM to align images from different sections and create a 3D reconstruction [237]. Finally, cross talk elimination improves the separation of channels by eliminating the unwanted cross-contamination of emission signals [183, 186]. The improvement of image contrast and resolution is achieved by techniques such as deconvolution [261], where a model or a measurement of microscope's diffraction effect are used to estimate the actual, diffraction-limited distribution of the signal.

Image preprocessing is usually followed by the recognition of the structures of interest, or so-called object segmentation, and—in the case of time series—generation of tracks of consecutive, connected positions for each object [262, 263]. The recognized objects may also be classified into different subsets according to some property of interest (such as the presence or absence of one or multiple fluorescent markers, the object roundness, or the object positioning with respect to another reference object). When performed correctly, these steps allow the automatic and reliable quantification of a specific set of features for each object, such as their area, volume, shape, or fluorescence content. Of note, the researcher should carefully assess real replicate independence when evaluating the statistical significance of these measurements [264].

In each of these steps, machine learning and deep learning methods—collectively called artificial intelligence methods—have proven useful [265], with the overall goal of making information extraction easier, more unbiased and inferring hidden parameters or dynamics.

7.1 | Machine-Learning Methods

Machine learning refers to the prediction capabilities acquired by an algorithm, either by fitting a set of model data or by identification of groups in a dataset with certain similarities. For example, one may train an algorithm to delineate the shape (i.e., segment) of all mitochondria in electron microscopy images or to identify, count and quantify the amount of material delivered to endolysosomes, which provides useful quantitative information on the endolysosomal trafficking activity inside the cell (Figure 3B). These machine-learning methodologies can be divided in two main classes, the supervised and the unsupervised methods. Supervised methods rely on provided information (i.e., ground-truth data, see Box 2) to learn about the task. This information is usually provided by data extracted with another technique or manually annotated. In supervised methods, so-called “feature based” or traditional machine learning methods and deep learning methods [266, 267] can be distinguished.

16000854, 2024, 10, Downloaded from https://onlinelibrary.wiley.com/doi/10.1111/tra.12957 by Biblioteca universitaria di Lugano, Wiley Online Library on [18/11/2024]. See the Terms and Conditions (https://onlinelibrary.wiley.com/terms-and-conditions) on Wiley Online Library for rules of use; OA articles are governed by the applicable Creative Commons License

BOX 2 | Vocabulary of current artificial intelligence methods in scientific image analysis.

Adversarial images. Images presenting patterns that can confound the deep learning model. These patterns can sometimes retrospectively be evident and recognizable (and thus avoidable by introducing some specific step before running the model), but they are many times very subtle and unpredictable.
Annotation. The process of generating a set of regions of interest (rectangles, points, precise contours) that identify the desired output of a trained model. These regions may also be divided according to a Classification and are often saved as Masks.
Classification. The separation of objects into different groups (classes) according to a specific Feature.
Convolution. A mathematical operation that sums the combinations of two functions, one running on the values of the other. This function has extensive applications in many fields, notably optics and deep learning. In optics, for example an image recorded by a microscope is always the convolution between the real sample pattern and the optical properties of the microscope, that is, a function describing the optical properties is run at each of the points of the sample to form the final image pattern. In the case of deep learning, neural network's layers are generated by convolving a certain function on the image to generate another image. This process, somewhat analogous to the generation of layers of abstraction in the mind, is the basis for CNNs.
Data augmentation. Data is often manipulated to generate more training data, like viewing the same image from different point of views may highlight different aspects. Images are often rotated, mirrored, or transformed with affine transformations.
Deconvolution. The best estimation of the true pattern of fluorescence molecules from an image, based on the optical properties of the acquisition instrument. As the final image is the Convolution of the true pattern of fluorescence molecules and the optical properties of the instrument, deconvolution is the inverse function. If well performed, the result is an image with higher resolution and higher contrast.
Feature. Each quantifiable value associated with a specific object. Examples are the area, perimeter, circularity, roughness or smoothness, fluorescence intensity in a specific channel inside the object, distance from another object or specific point and so forth.
Ground-truth data. Data, which refers to the correct answer for the specific question. For example, in the case of image segmentation, it is a mask outlining the true shape of an object to be segmented. The ideal output of a machine-learning model would be a result equal to ground-truth data.
Hallucination. The generation of plausible but incorrect output data. The output of deep learning models is expressed under the hood as a probability of the predicted outcome, which is then cut into a clear answer by a thresholding algorithm. Although models are trained to optimize this output answer, one should always keep in mind that deep learning models will always have some degree of randomness.
Mask. An image where each pixel represents a TRUE/FALSE statement. For example, pixel may be classified into belonging to an object of interest versus background. These masks are often the result of an Annotation when provided as training information along with the corresponding images. Sometimes a mask can be a set of discrete numbers, each corresponding to a certain class of objects (see Classification).
Neural network. Neural networks are composed of layers. Starting from an input layer, images are processed in many "hidden" layers until the output is given in the output layer. At each layer a mathematical operation is performed (such as a Convolution, in convolutional neural networks or CNNs for short). Layers are connected by function with parameters—also called weights—that are optimized during training.
Segmentation. The process of recognizing the boundaries of an object, thus distinguishing an object from another.
Supervised learning. A model trained by providing input data and the desired outcome (e.g., Annotations). Supervised learning is often used to match as close as possible human recognition.
Training. The process of optimizing a set of weights for the neural network parameters so that it matches as closely as possible the input data and the desired outcome (such as an Annotation or an output image). Mathematically, this is often solved as an iterative process of minimization, where the quantity to be minimized is a measure of the distance between some annotated images and their corresponding annotation.
Unsupervised learning. A model trained without providing any Annotation. Unsupervised learning can be used for example for imaginative tasks, such as the generation of images where the outcome cannot be stated precisely. Although supervised and unsupervised may be seen as opposites, some tasks may require the use of both [293–295].

In "feature based" machine learning, a set of quantifiable "features" (such as the area, perimeter, shape parameters or contrast with the surrounding pixels) is defined beforehand by the researcher from representative images and then weighted by the computer, based on input images and segmentations, to generate an algorithm that matches as closely as possible the training data. For example, these techniques have been applied to generate a model that recognizes cells with clustered or distributed lysosomes in high throughput experiments [268]. In contrast, in the case of deep learning, the researcher first defines a neuronal network architecture, with a specific set of operations on input images and a structure of connections between each image operation, thus mimicking the connection between neurons. This structure is usually defined in levels, each level extracting a deeper level of abstraction from the data (hence the name "deep learning"). Once the architecture is defined, each image is rotated or modified to generate more information and improve the quality of results (data augmentation). Among the possible operations used in image analysis to extract different levels of information, the most common one is "convolution" (see Box 2). A network architecture that uses this type of operation is called Convolutional Neural Network (CNN). The results of the combination of these operations are weighted by a linear combination between each connection, and the network training is essentially a problem of minimizing all these coefficients (sometimes in the range of billions). Thus, deep learning provides a denser, richer,

16000854, 2024, 10, Downloaded from https://onlinelibrary.wiley.com/doi/10.1111/tra.12957 by Biblioteca universitaria di Lugano, Wiley Online Library on [18/11/2024]. See the Terms and Conditions (https://onlinelibrary.wiley.com/terms-and-conditions) on Wiley Online Library for rules of use; OA articles are governed by the applicable Creative Commons License

and more accurate model than feature-based machine learning methods for image recognition [269, 270] but requires extensive computing resources to be trained. In image acquisition, supervised deep learning has been used to reduce photodamage in structured illumination microscopy [271] and denoise data from electron microscopy [272].

In opposition to supervised machine learning methods, unsupervised methods identify and extract common patterns from given data without being provided any annotation [266], using an algorithm that clusters data according to common features or by training of a deep learning model. In the latter case, input data are often not selected sample images, but simulated ground-truth data. In image acquisition, unsupervised methods have been used for restoring or improving image quality in situations where the acquisition of ground-truth images is impossible [273–276] or as an alternative to deconvolution methods [277–279].

7.2 | Deep Learning Tools to Analyze Autophagic Flux and Lysosomal Protein Trafficking

Current methods directly employing deep learning for the determination of autophagic flux address the identification of autophagic phenotypes of yeast cells upon knockout of *atg* genes by confocal microscopy images [280] and segmentation of lysosomes for the unbiased classification of their cargo content and quantification of their features [281]. General tools also provide deep learning frameworks, which can then be trained and used in specific image segmentation tasks [282–284], or for helping in registration of correlative EM images [285]. Proteolytic HaloTag reporter in combination with deep learning segmentation has been recently applied by our group to evaluate the lysosomal trafficking efficiency of LSD-linked misfolded mutant enzymes [80]. Moreover, efforts are ongoing to develop machine learning data mining to aggregate existing information on targets for LSDs and available compounds to suggest new molecules with therapeutic potential [286]. Another useful application of these tools would be the integration of automatic quantification of tandem-fluorescent reporters (such as the mentioned HaloTag-GFP or mCherry-GFP reporters [287]). With these tools, researchers could quantify material delivered to endolysosomes, compare the experimental condition with an appropriate known negative control, and extract ratiometric information on delivered versus non-delivered material in the same sample, such as when quantifying the proportion of organelles or misfolded polypetides delivered to endolysosomes.

Some considerations about the limitations of deep learning techniques must be discussed. As mentioned, deep learning models currently require extensive resources and time to be trained. In addition, the generation of input data, the generation of ground truth information, and the choice of the correct architecture all contribute to increased time needed for the training of a reliable network. Recent advances in artificial intelligence are making it easier and cheaper to train models and integrate them into pipelines [284, 288], however, wide-scale integration into trafficking research and the ease-of-use for non-experts are yet to achieve. Still, a good training outcome does not guarantee an error-free performance, as the problems of hallucination [289] or adversarial images [290] often persist. As unsupervised methods extrapolate their own understanding of input data without any ground truth information, it should also be noted that in some cases the link between the recognized features and biologically relevant variables may not be evident or misleading, or just not useful: for example, clustering algorithms try to identify groups within a dataset (such as the number, size, location or amount of fluorescence signal inside each endolysosome in a cell) according to their differences, while these groups might end up having little or difficult-to-explain biological meaning. On the other hand, exploring unsupervised models or weakly supervised models might reduce our reliance on the time-consuming generation of labeled ground-truth data [289].

After feature extraction, the analysis of the generated data can take advantage of machine-learning or deep-learning-enhanced bioinformatics analysis. Combining this information with data mining techniques such as those developed for genomics or proteomics [291] could be useful in exploring complex data, such as identifying and validating novel autophagy players or finding new correlations between autophagy and diseases [292]. Prospectively, the above-mentioned microscopy tools together with deep-learning-based analyses will allow the unbiased analysis and the employment of these techniques in high-throughput small molecule and genetic screenings for the discovery of potential drug targets and candidates, in a deep-learning-informed cell biology.

8 | Future Directions and Conclusion

The use of fluorescent reporters that change their physicochemical properties when they arrive/are delivered in acidic degradative compartments is quickly expanding within the field of autophagy, as well as seeping into the domains of lysosomal trafficking and endocytosis. A vast palette of single and tandem reporters is available to the researchers, providing multiple and complementary usage (endogenous and ectopic tagging) and readout modalities (light and electron microscopy, in-gel fluorescence, western blot and flow cytometry, Figure 2). In the future, we expect that the effort on continued development and refinement of fluorescent reporters will be dictated by the technical constraints that are still not addressed in these fields. These technical requirements in autophagy research currently include, among others, the genetic incorporation of fluorescent reporters into the genome for tagging endogenous gene products in cell lines and laboratory animals. The design of reporters will focus on novel fluorescent proteins with high brightness, reduced molecular weight to facilitate genome integration, low cytotoxicity, and reduced interference with the function of the tagged protein and with the pathway under investigation.

In the field of protein misfolding and rare LSDs, systems reliably reporting on the arrival of mutant polypeptides to lysosomal compartments are still in their infancy. As demonstrated for mCherry-GFP [174, 175] and the HaloTag-based reporters [76, 80], fluorescent reporters may be used for lysosomal enzyme and misfolded protein trafficking research. Importantly, the transitioning of fluorescent reporters from the role of a pure academic tool into industrial drug discovery pipelines would bolster the implementation of scalable high-throughput readouts and pipelines with automated data analysis. The ability to quantify precisely, quickly and in high-throughput fashion the

16000854, 2024, 10, Downloaded from https://onlinelibrary.wiley.com/doi/10.1111/tra.12957 by Biblioteca universitaria di Lugano, Wiley Online Library on [18/11/2024]. See the Terms and Conditions (https://onlinelibrary.wiley.com/terms-and-conditions) on Wiley Online Library for rules of use; OA articles are governed by the applicable Creative Commons License

trafficking efficiency of degradative substrates and lysosomal enzymes is crucial for the identification of effective chemical or pharmacological modulators of lysosomal trafficking [115, 177].

The parallel advancement of fluorescent probe engineering and image acquisition techniques will provide a deeper view of trafficking events. In particular, the application of super-resolution techniques to obtain structural (cryo electron microscopy), spatial (fixed cell imaging), and dynamical (live cell imaging) information is still in the early stages. The resolution improvement in immunofluorescence microscopy will also benefit correlative light-electron microscopy investigations, allowing the definition of structures of interest with greater confidence and greater detail, while the development and more extensive application of higher-resolution and faster volume EM techniques, such as cryo-ET, will increase our three-dimensional understanding of the autophagic events. The integration of time-resolved HaloTag pulse-chase techniques with the EM, for example, using 3,3′-diaminodbenzidine (DAB) precipitation [81, 296], will provide temporal information at the EM resolution. The combination of cryo-fixation techniques with fluorescence live cell imaging (either conventional or super-resolution) will help in spotting right-in-time events by quickly passing from live cell imaging to the cryo-fixed sample.

Commercial systems are progressively increasing the use of machine learning techniques in analysis and recently also in the image acquisition phase, with the goal of automating acquisition and identification of common and rare events. The development of more dedicated applications of machine learning techniques to the field will facilitate the unbiased analysis, simplifying the analysis of large number of cells and—when their statistical interpretation is appropriately handled—adding confidence to quantitative analyses. As the amount of information grows with more complex techniques, relying on automation is becoming increasingly important.

All in all, integrating visualization of protein and organelle delivery events to degradative compartments, data acquisition with high throughput, high resolution and time-resolved microscopy, and analysis automation with machine learning-assisted technologies will allow identification, characterization, and development of effective therapeutic compounds for lysosomal trafficking and autophagy-associated disorders.

Acknowledgments

We thank the members of Molinari's laboratory for discussions, and critical reading of the manuscript. Open access funding provided by Universita della Svizzera italiana.

Ethics Statement

The authors have nothing to report.

Conflicts of Interest

The authors declare no conflicts of interest.

Peer Review

The peer review history for this article is available at https://www.webofscience.com/api/gateway/wos/peer-review/10.1111/tra.12957.

References

1. E. Metchinkoff, *Leçons sur la Pathologie Comparée de l'Inflammation: Faites à l'Institut Pasteur en Avril et Mai 1891* (Paris, France: Libraire de l'Académie de Médecine, 1892).

2. J. Berthet and C. de Duve, "Tissue Fractionation Studies. I. The Existence of a Mitochondria-Linked, Enzymically Inactive Form of Acid Phosphatase in Rat-Liver Tissue," *Biochemical Journal* 50, no. 2 (1951): 174–181.

3. J. Berthet, L. Berthet, F. Appelmans, and C. De Duve, "Tissue Fractionation Studies. II. The Nature of the Linkage Between Acid Phosphatase and Mitochondria in Rat-Liver Tissue," *Biochemical Journal* 50, no. 2 (1951): 182–189.

4. C. de Duve, B. C. Pressman, R. Gianetto, R. Wattiaux, and F. Appelmans, "Tissue Fractionation Studies. 6. Intracellular Distribution Patterns of Enzymes in Rat-Liver Tissue," *Biochemical Journal* 60, no. 4 (1955): 604–617.

5. F. Appelmans, R. Wattiaux, and C. de Duve, "Tissue Fractionation Studies. 5. The Association of Acid Phosphatase With a Special Class of Cytoplasmic Granules in Rat Liver," *Biochemical Journal* 59, no. 3 (1955): 438–445.

6. A. B. Novikoff, H. Beaufay, and C. de Duve, "Electron Microscopy of Lysosomerich Fractions From Rat Liver," *Journal of Biophysical and Biochemical Cytology* 2, no. 4 Suppl (1956): 179–184.

7. H. R. Shin and R. Zoncu, "The Lysosome at the Intersection of Cellular Growth and Destruction," *Developmental Cell* 54, no. 2 (2020): 226–238.

8. A. Ballabio and J. S. Bonifacino, "Lysosomes as Dynamic Regulators of Cell and Organismal Homeostasis," *Nature Reviews. Molecular Cell Biology* 21, no. 2 (2019): 101–118.

9. J. Huotari and A. Helenius, "Endosome Maturation," *EMBO Journal* 30, no. 17 (2011): 3481–3500.

10. W. W. Yim and N. Mizushima, "Lysosome Biology in Autophagy," *Cell Discovery* 6 (2020): 1–12.

11. N. A. Bright, L. J. Davis, and J. P. Luzio, "Endolysosomes Are the Principal Intracellular Sites of Acid Hydrolase Activity," *Current Biology* 26, no. 17 (2016): 2233–2245.

12. S. Okhuma and B. Poole, "Fluorescence Probe Measurement of the Intralysosomal pH in Living Cells and the Pertubation of pH by Various Agents," *Proceedings of the National Academy of Sciences of the United States of America* 75 (1978): 3327–3331.

13. O. D. Hensens, R. L. Monaghan, L. Y. Huang, and G. Albersschonberg, "Structure of the Sodium and Potassium-Ion Activated Adenosine-Triphosphatase Inhibitor-L-681110," *Journal of the American Chemical Society* 105, no. 11 (1983): 3672–3679.

14. E. J. Bowman, A. Siebers, and K. Altendorf, "Bafilomycins: A Class of Inhibitors of Membrane ATPases From Microorganisms, Animal Cells, and Plant Cells," *National Academy of Sciences of the United States of America* 85, no. 21 (1988): 7972–7976.

15. J. T. Woo, C. Shinohara, K. Sakai, K. Hasumi, and A. Endo, "Isolation, Characterization and Biological-Activities of Concanamycins as Inhibitors of Lysosomal Acidification," *Journal of Antibiotics* 45, no. 7 (1992): 1108–1116.

16. M. Taipale, "Disruption of Protein Function by Pathogenic Mutations: Common and Uncommon Mechanisms," *Biochemistry and Cell Biology* 97, no. 1 (2019): 46–57.

17. K. Yoshida, A. Oshima, M. Shimmoto, et al., "Human Beta-Galactosidase Gene Mutations in GM1-Gangliosidosis: A Common Mutation Among Japanese Adult/Chronic Cases," *American Journal of Human Genetics* 49, no. 2 (1991): 435–442.

18. I. Bendikov-Bar, I. Ron, M. Filocamo, and M. Horowitz, "Characterization of the ERAD Process of the L444P Mutant

16000854, 2024, 10, Downloaded from https://onlinelibrary.wiley.com/doi/10.1111/tra.12957 by Biblioteca universitaria di Lugano, Wiley Online Library on [18/11/2024]. See the Terms and Conditions (https://onlinelibrary.wiley.com/terms-and-conditions) on Wiley Online Library for rules of use; OA articles are governed by the applicable Creative Commons License

Glucocerebrosidase Variant," *Blood Cells, Molecules & Diseases* 46, no. 1 (2011): 4–10.

19. D. Hofer, K. Paul, K. Fantur, et al., "GM1 Gangliosidosis and Morquio B Disease: Expression Analysis of Missense Mutations Affecting the Catalytic Site of Acid Beta-Galactosidase," *Human Mutation* 30, no. 8 (2009): 1214–1221.

20. M. L. Schultz, K. L. Krus, S. Kaushik, et al., "Coordinate Regulation of Mutant NPC1 Degradation by Selective ER Autophagy and MARCH6-Dependent ERAD," *Nature Communications* 9, no. 1 (2018): 3671.

21. A. Marazza, C. Galli, E. Fasana, et al., "Endoplasmic Reticulum and Lysosomal Quality Control of Four Nonsense Mutants of Iduronate 2-Sulfatase Linked to Hunter's Syndrome," *DNA and Cell Biology* 39, no. 2 (2020): 226–234.

22. A. Sanchez-Martinez, M. Beavan, M. E. Gegg, K.-Y. Chau, A. J. Whitworth, and A. H. V. Schapira, "Parkinson Disease-Linked GBA Mutation Effects Reversed by Molecular Chaperones in Human Cell and Fly Models," *Scientific Reports* 6, no. 1 (2016): 31380.

23. D. M. Pereira, P. Valentão, and P. B. Andrade, "Tuning Protein Folding in Lysosomal Storage Diseases: The Chemistry Behind Pharmacological Chaperones," *Chemical Science* 9, no. 7 (2018): 1740–1752.

24. J. C. Losada Díaz, J. Cepeda Del Castillo, E. A. Rodriguez-López, and C. J. Alméciga-Díaz, "Advances in the Development of Pharmacological Chaperones for the Mucopolysaccharidoses," *International Journal of Molecular Sciences* 21, no. 1 (2019): 232.

25. L. Liguori, M. Monticelli, M. Allocca, et al., "Pharmacological Chaperones: A Therapeutic Approach for Diseases Caused by Destabilizing Missense Mutations," *International Journal of Molecular Sciences* 21, no. 2 (2020): 489.

26. A. B. Novikoff, "Lysosomes and Related Particles," in *The Cell*, vol. II, ed. J. B. A. E. Mirsky (New York, NY: Academic Press, 1961), 423–488.

27. C. de Duve and R. Wattiaux, "Functions of Lysosomes," *Annual Review of Physiology* 28 (1966): 435–492.

28. W. A. Dunn, A. L. Hubbard, and N. N. Aronson, "Low Temperature Selectively Inhibits Fusion Between Pinocytic Vesicles and Lysosomes During Heterophagy of 125I-Asialofetuin by the Perfused Rat Liver," *Journal of Biological Chemistry* 255, no. 12 (1980): 5971–5978.

29. S. Mayor and R. E. Pagano, "Pathways of Clathrin-Independent Endocytosis," *Nature Reviews. Molecular Cell Biology* 8, no. 8 (2007): 603–612.

30. J. A. Swanson and C. Watts, "Macropinocytosis," *Trends in Cell Biology* 5, no. November (1995): 424–428.

31. J. A. Swanson and J. S. King, "The Breadth of Macropinocytosis Research," *Philosophical Transactions of the Royal Society, B: Biological Sciences* 374, no. 1765 (2019): 20180146.

32. R. G. Parton, "Caveolae: Structure, Function, and Relationship to Disease," *Annual Review of Cell and Developmental Biology* 34, no. 1 (2018): 111–136.

33. C. Matthaeus and J. W. Taraska, "Energy and Dynamics of Caveolae Trafficking," *Frontiers in Cell and Developmental Biology* 8 (2021): 614472.

34. C. Pathak, F. U. Vaidya, B. N. Waghela, et al., "Insights of Endocytosis Signaling in Health and Disease," *International Journal of Molecular Sciences* 24, no. 3 (2023): 2971.

35. B. Han, C. A. Copeland, Y. Kawano, et al., "Characterization of a Caveolin-1 Mutation Associated With Both Pulmonary Arterial Hypertension and Congenital Generalized Lipodystrophy," *Traffic* 17, no. 12 (2016): 1297–1312.

36. C. A. Copeland, B. Han, A. Tiwari, et al., "A Disease-Associated Frameshift Mutation in Caveolin-1 Disrupts Caveolae Formation and Function Through Introduction of a De Novo ER Retention Signal," *Molecular Biology of the Cell* 28, no. 22 (2017): 3095–3111.

37. Y. K. Hayashi, C. Matsuda, M. Ogawa, et al., "Human PTRF Mutations Cause Secondary Deficiency of Caveolins Resulting in Muscular Dystrophy With Generalized Lipodystrophy," *Journal of Clinical Investigation* 119, no. 9 (2009): 2623–2633.

38. T. Andrews and K. E. Sullivan, "Infections in Patients With Inherited Defects in Phagocytic Function," *Clinical Microbiology Reviews* 16, no. 4 (2003): 597–621.

39. B. Banushi, S. R. Joseph, B. Lum, J. J. Lee, and F. Simpson, "Endocytosis in Cancer and Cancer Therapy," *Nature Reviews. Cancer* 23, no. 7 (2023): 450–473.

40. F. Reggiori and M. Molinari, "ER-Phagy: Mechanisms, Regulation, and Diseases Connected to the Lysosomal Clearance of the Endoplasmic Reticulum," *Physiological Reviews* 102, no. 3 (2022): 1393–1448.

41. S. Ferro-Novick, F. Reggiori, and J. L. Brodsky, "ER-Phagy, ER Homeostasis, and ER Quality Control: Implications for Disease," *Trends in Biochemical Sciences* 46, no. 8 (2021): 630–639.

42. I. Dikic and Z. Elazar, "Mechanism and Medical Implications of Mammalian Autophagy," *Nature Reviews. Molecular Cell Biology* 19, no. 6 (2018): 349–364.

43. P. Grumati, I. Dikic, and A. Stolz, "ER-Phagy at a Glance," *Journal of Cell Science* 131, no. 17 (2018): 1–6.

44. A. Stolz and P. Grumati, "The Various Shades of ER-Phagy," *FEBS Journal* 286, no. 23 (2019): 4642–4649.

45. T. Lamark and T. Johansen, "Mechanisms of Selective Autophagy," *Annual Review of Cell and Developmental Biology* 37 (2021): 1–27.

46. S. Wilkinson, "ER-Phagy: Shaping Up and Destressing the Endoplasmic Reticulum," *FEBS Journal* 286, no. 14 (2019): 2645–2663.

47. K. Mochida and H. Nakatogawa, "ER-Phagy: Selective Autophagy of the Endoplasmic Reticulum," *EMBO Reports* 23, no. 8 (2022): e55192.

48. J. A. Schafer and S. Schuck, "ESCRTing Endoplasmic Reticulum to Microautophagic Degradation," *Autophagy* 16, no. 4 (2020): 763–764.

49. S. Schuck, "Microautophagy—Distinct Molecular Mechanisms Handle Cargoes of Many Sizes," *Journal of Cell Science* 133, no. 17 (2020): jcs246322.

50. H. Chino and N. Mizushima, "ER-Phagy: Quality Control and Turnover of Endoplasmic Reticulum," *Trends in Cell Biology* 30, no. 5 (2020): 384–398.

51. Y. Lei and D. J. Klionsky, "The Emerging Roles of Autophagy in Human Diseases," *Biomedicine* 9, no. 11 (2021): 1651.

52. D. J. Klionsky, G. Petroni, R. K. Amaravadi, et al., "Autophagy in Major Human Diseases," *EMBO Journal* 40, no. 19 (2021): e108863.

53. A. Picca, J. Faitg, J. Auwerx, L. Ferrucci, and D. D'Amico, "Mitophagy in Human Health, Ageing and Disease," *Nature Metabolism* 5, no. 12 (2023): 2047–2061.

54. C. A. Homewood, D. C. Warhurst, W. Peters, and V. C. Baggaley, "Lysosomes, pH and the Anti-Malarial Action of Chloroquine," *Nature* 235, no. 5332 (1972): 50–52.

55. J. Glickman, K. Croen, S. Kelly, and Q. Al-Awqati, "Golgi Membranes Contain an Electrogenic H+ Pump in Parallel to a Chloride Conductance," *Journal of Cell Biology* 97, no. 4 (1984): 1303–1308.

56. P. Paroutis, N. Touret, and S. Grinstein, "The pH of the Secretory Pathway: Measurement, Determinants, and Regulation," *Physiology* 19, no. 4 (2004): 207–215.

57. A. E. Smith and A. Helenius, "How Viruses Enter Animal Cells," *Science* 304, no. 5668 (2004): 237–242.

16000854, 2024, 10, Downloaded from https://onlinelibrary.wiley.com/doi/10.1111/tra.12957 by Biblioteca universitaria di Lugano, Wiley Online Library on [18/11/2024]. See the Terms and Conditions (https://onlinelibrary.wiley.com/terms-and-conditions) on Wiley Online Library for rules of use; OA articles are governed by the applicable Creative Commons License

58. S. Padilla-Parra, P. M. Matos, N. Kondo, M. Marin, N. C. Santos, and G. B. Melikyan, "Quantitative Imaging of Endosome Acidification and Single Retrovirus Fusion With Distinct Pools of Early Endosomes," *National Academy of Sciences of the United States of America* 109, no. 43 (2012): 17627–17632.

59. T. Yadati, T. Houben, A. Bitorina, and R. Shiri-Sverdlov, "The Ins and Outs of Cathepsins: Physiological Function and Role in Disease Management," *Cells* 9, no. 7 (2020): 1679.

60. J. L. Goldstein, G. Y. Brunschede, and M. S. Brown, "Inhibition of Proteolytic Degradation of Low Density Lipoprotein in Human Fibroblasts by Chloroquine, Concanavalin A, and Triton WR 1339," *Journal of Biological Chemistry* 250, no. 19 (1975): 7854–7862.

61. A. H. Mackenzie, "Pharmacologic Actions of 4-Aminoquinoline Compounds," *American Journal of Medicine* 75, no. 1a (1983): 5–10.

62. C. J. Jones and M. I. Jayson, "Chloroquine: Its Effect on Leucocyte Auto- and Heterophagocytosis," *Annals of the Rheumatic Diseases* 43, no. 2 (1984): 205–212.

63. C. J. Jones, R. S. Salisbury, and M. I. Jayson, "The Presence of Abnormal Lysosomes in Lymphocytes and Neutrophils During Chloroquine Therapy: A Quantitative Ultrastructural Study," *Annals of the Rheumatic Diseases* 43, no. 5 (1984): 710–715.

64. M. Mauthe, I. Orhon, C. Rocchi, et al., "Chloroquine Inhibits Autophagic Flux by Decreasing Autophagosome-Lysosome Fusion," *Autophagy* 14, no. 8 (2018): 1435–1455.

65. I. Tanida, T. Ueno, and E. Kominami, "LC3 Conjugation System in Mammalian Autophagy," *International Journal of Biochemistry & Cell Biology* 36, no. 12 (2004): 2503–2518.

66. I. Tanida, N. Minematsu-Ikeguchi, T. Ueno, and E. Kominami, "Lysosomal Turnover, But Not a Cellular Level, of Endogenous LC3 Is a Marker for Autophagy," *Autophagy* 1, no. 2 (2005): 84–91.

67. N. Mizushima and T. Yoshimori, "How to Interpret LC3 Immunoblotting," *Autophagy* 3, no. 6 (2007): 542–545.

68. N. Yuan, L. Song, S. Zhang, et al., "Bafilomycin A1 Targets Both Autophagy and Apoptosis Pathways in Pediatric B-Cell Acute Lymphoblastic Leukemia," *Haematologica* 100, no. 3 (2015): 345–356.

69. R. Köchl, X. W. Hu, E. Y. W. Chan, and S. A. Tooze, "Microtubules Facilitate Autophagosome Formation and Fusion of Autophagosomes With Endosomes," *Traffic* 7, no. 2 (2006): 129–145.

70. O. Florey, N. Gammoh, S. E. Kim, X. Jiang, and M. Overholtzer, "V-ATPase and Osmotic Imbalances Activate Endolysosomal LC3 Lipidation," *Autophagy* 11, no. 1 (2015): 88–99.

71. E. Jacquin, S. Leclerc-Mercier, C. Judon, E. Blanchard, S. Fraitag, and O. Florey, "Pharmacological Modulators of Autophagy Activate a Parallel Noncanonical Pathway Driving Unconventional LC3 Lipidation," *Autophagy* 13, no. 5 (2017): 854–867.

72. G. V. Los, L. P. Encell, M. G. McDougall, et al., "HaloTag: A Novel Protein Labeling Technology for Cell Imaging and Protein Analysis," *ACS Chemical Biology* 3, no. 6 (2008): 373–382.

73. C. G. England, H. M. Luo, and W. B. Cai, "HaloTag Technology: A Versatile Platform for Biomedical Applications," *Bioconjugate Chemistry* 26, no. 6 (2015): 975–986.

74. S. Kimura, T. Noda, and T. Yoshimori, "Dissection of the Autophagosome Maturation Process by a Novel Reporter Protein, Tandem Fluorescent-Tagged LC3," *Autophagy* 3, no. 5 (2007): 452–460.

75. S. Pankiv, T. H. Clausen, T. Lamark, et al., "p62/SQSTM1 Binds Directly to Atg8/LC3 to Facilitate Degradation of Ubiquitinated Protein Aggregates by Autophagy," *Journal of Biological Chemistry* 282, no. 33 (2007): 24131–24145.

76. M. Rudinskiy, T. J. Bergmann, and M. Molinari, "Quantitative and Time-Resolved Monitoring of Organelle and Protein Delivery to the Lysosome With A Tandem Fluorescent Halo-GFP Reporter," *Molecular Biology of the Cell* 33, no. 6 (2022): ar57.

77. W. W.-Y. Yim, H. Yamamoto, and N. Mizushima, "A Pulse-Chasable Reporter Processing Assay for Mammalian Autophagic Flux With HaloTag," *eLife* 11 (2022): e78923.

78. C. Zhou, W. Zhong, J. Zhou, et al., "Monitoring Autophagic Flux by an Improved Tandem Fluorescent-Tagged LC3 (mTagRFP-mWasabi-LC3) Reveals That High-Dose Rapamycin Impairs Autophagic Flux in Cancer Cells," *Autophagy* 8, no. 8 (2012): 1215–1226.

79. J. R. Liang, E. Lingeman, S. Ahmed, and J. E. Corn, "Atlastins Remodel the Endoplasmic Reticulum for Selective Autophagy," *Journal of Cell Biology* 217, no. 10 (2018): 3354–3367.

80. M. Rudinskiy, M. Pons-Vizcarra, T. Soldà, et al., "Validation of a Highly Sensitive HaloTag-Based Assay to Evaluate the Potency of a Novel Class of Allosteric β-Galactosidase Correctors," *PLoS One* 18, no. 11 (2023): e0294437.

81. M. Rudinskiy and M. Molinari, "Tandem Fluorescent Halo-GFP Reporter for Quantitative and Time-Resolved Monitoring of Organelle and Protein Delivery to Lysosomes," *Autophagy Reports* 1 (2022): 187–191.

82. H. Chino, T. Hatta, T. Natsume, and N. Mizushima, "Intrinsically Disordered Protein TEX264 Mediates ER-Phagy," *Molecular Cell* 74, no. 5 (2019): 909–921.e906.

83. H. Katayama, T. Kogure, N. Mizushima, T. Yoshimori, and A. Miyawaki, "A Sensitive and Quantitative Technique for Detecting Autophagic Events Based on Lysosomal Delivery," *Chemistry & Biology* 18, no. 8 (2011): 1042–1052.

84. H. Katayama, H. Hama, K. Nagasawa, et al., "Visualizing and Modulating Mitophagy for Therapeutic Studies of Neurodegeneration," *Cell* 181, no. 5 (2020): 1176–1187.e1116.

85. D. J. Klionsky, "For the Last Time, It Is GFP-Atg8, Not Atg8-GFP (And the Same Goes for LC3)," *Autophagy* 7, no. 10 (2011): 1093–1094.

86. H. Shinoda, M. Shannon, and T. Nagai, "Fluorescent Proteins for Investigating Biological Events in Acidic Environments," *International Journal of Molecular Sciences* 19, no. 6 (2018): 1548.

87. N. V. dos Santos, C. F. Saponi, T. M. Ryan, F. L. Primo, T. L. Greaves, and J. F. B. Pereira, "Reversible and Irreversible Fluorescence Activity of the Enhanced Green Fluorescent Protein in pH: Insights for the Development of pH-Biosensors," *International Journal of Biological Macromolecules* 164 (2020): 3474–3484.

88. H. Katayama, A. Yamamoto, N. Mizushima, T. Yoshimori, and A. Miyawaki, "GFP-Like Proteins Stably Accumulate in Lysosomes," *Cell Structure and Function* 33, no. 1 (2008): 1–12.

89. B. N. Giepmans, S. R. Adams, M. H. Ellisman, and R. Y. Tsien, "The Fluorescent Toolbox for Assessing Protein Location and Function," *Science* 312, no. 5771 (2006): 217–224.

90. E. A. Rodriguez, R. E. Campbell, J. Y. Lin, et al., "The Growing and Glowing Toolbox of Fluorescent and Photoactive Proteins," *Trends in Biochemical Sciences* 42, no. 2 (2017): 111–129.

91. N. C. Shaner, R. E. Campbell, P. A. Steinbach, B. N. Giepmans, A. E. Palmer, and R. Y. Tsien, "Improved Monomeric Red, Orange and Yellow Fluorescent Proteins Derived From *Discosoma* sp. Red Fluorescent Protein," *Nature Biotechnology* 22, no. 12 (2004): 1567–1572.

92. I. Tanida, T. Ueno, and Y. Uchiyama, "A Super-Ecliptic, pHluorin-mKate2, Tandem Fluorescent Protein-Tagged Human LC3 for the Monitoring of Mammalian Autophagy," *PLoS One* 9, no. 10 (2014): e110600.

93. I. Tanida, T. Ueno, and Y. Uchiyama, "Use of pHlurorin-mKate2-Human LC3 to Monitor Autophagic Responses," *Methods in Enzymology* 587 (2017): 87–96.

16000854, 2024, 10, Downloaded from https://onlinelibrary.wiley.com/doi/10.1111/tra.12957 by Biblioteca universitaria di Lugano, Wiley Online Library on [18/11/2024]. See the Terms and Conditions (https://onlinelibrary.wiley.com/terms-and-conditions) on Wiley Online Library for rules of use; OA articles are governed by the applicable Creative Commons License

94. H. Kim, J. Choi, K. S. Inn, and J. Seong, "Visualization of Autophagy Progression by a Red-Green-Blue Autophagy Sensor," *ACS Sensors* 5, no. 12 (2020): 3850–3861.

95. H. W. Ai, K. L. Hazelwood, M. W. Davidson, and R. E. Campbell, "Fluorescent Protein FRET Pairs for Ratiometric Imaging of Dual Biosensors," *Nature Methods* 5, no. 5 (2008): 401–403.

96. D. Shcherbo, S. C. Murphy, G. V. Ermakova, et al., "Far-Red Fluorescent Tags for Protein Imaging in Living Tissues," *Biochemical Journal* 418, no. 3 (2009): 567–574.

97. L. K. Hein, P. M. Apaja, K. Hattersley, et al., "A Novel Fluorescent Probe Reveals Starvation Controls the Commitment of Amyloid Precursor Protein to the Lysosome," *Biochimica et Biophysica Acta-Molecular Cell Research* 1864, no. 10 (2017): 1554–1565.

98. Z.-Y. Li, Y.-L. Shi, G.-X. Liang, et al., "Visualization of GLUT1 Trafficking in Live Cancer Cells by the Use of a Dual-Fluorescence Reporter," *ACS Omega* 5, no. 26 (2020): 15911–15921.

99. L. Huang, D. Pike, D. E. Sleat, V. Nanda, and P. Lobel, "Potential Pitfalls and Solutions for Use of Fluorescent Fusion Proteins to Study the Lysosome," *PLoS One* 9, no. 2 (2014): e88893.

100. H. An and J. W. Harper, "Systematic Analysis of Ribophagy in Human Cells Reveals Bystander Flux During Selective Autophagy," *Nature Cell Biology* 20, no. 2 (2018): 135–143.

101. I. Fregno, E. Fasana, T. J. Bergmann, et al., "ER-to-Lysosome-Associated Degradation of Proteasome-Resistant ATZ Polymers Occurs via Receptor-Mediated Vesicular Transport," *EMBO Journal* 37, no. 17 (2018): e99259.

102. H. Hayashi, T. Wang, M. Tanaka, et al., "Monitoring the Autophagy-Endolysosomal System Using Monomeric Keima-Fused MAP1LC3B," *PLoS One* 15, no. 6 (2020): e0234180.

103. N. Engedal, T. Sønstevold, C. J. Beese, et al., "Measuring Autophagic Cargo Flux With Keima-Based Probes," *Methods in Molecular Biology* 2445 (2022): 99–115.

104. J. H. Um, Y. Y. Kim, T. Finkel, and J. Yun, "Sensitive Measurement of Mitophagy by Flow Cytometry Using the pH-Dependent Fluorescent Reporter Mt-Keima," *Journal of Visualized Experiments* 138 (2018): 58099.

105. M. Lazarou, D. A. Sliter, L. A. Kane, et al., "The Ubiquitin Kinase PINK1 Recruits Autophagy Receptors to Induce Mitophagy," *Nature* 524, no. 7565 (2015): 309–314.

106. F. G. Barone, S. Urbé, and M. J. Clague, "Segregation of Pathways Leading to Pexophagy," *Life Science Alliance* 6, no. 5 (2023): e202201825.

107. H. An, A. Ordureau, M. Körner, J. A. Paulo, and J. W. Harper, "Systematic Quantitative Analysis of Ribosome Inventory During Nutrient Stress," *Nature* 583, no. 7815 (2020): 303–309.

108. D. J. Klionsky, A. K. Abdel-Aziz, S. Abdelfatah, et al., "Guidelines for the Use and Interpretation of Assays for Monitoring Autophagy (4th Edition)," *Autophagy* 17, no. 1 (2021): 1–382.

109. S. Karasawa, T. Araki, M. Yamamoto-Hino, and A. Miyawaki, "A Green-Emitting Fluorescent Protein From Galaxeidae Coral and Its Monomeric Version for Use in Fluorescent Labeling," *Journal of Biological Chemistry* 278, no. 36 (2003): 34167–34171.

110. A. W. Nguyen and P. S. Daugherty, "Evolutionary Optimization of Fluorescent Proteins for Intracellular FRET," *Nature Biotechnology* 23, no. 3 (2005): 355–360.

111. N. Jimenez-Moreno, C. Salomo-Coll, L. C. Murphy, and S. Wilkinson, "Signal-Retaining Autophagy Indicator as a Quantitative Imaging Method for ER-Phagy," *Cells* 12, no. 8 (2023): 1134.

112. N. Engedal and P. O. Seglen, "Autophagy of Cytoplasmic Bulk Cargo Does Not Require LC3," *Autophagy* 12, no. 2 (2016): 439–441.

113. A. E. Ohnstad, J. M. Delgado, B. J. North, et al., "Receptor-Mediated Clustering of FIP200 Bypasses the Role of LC3 Lipidation in Autophagy," *EMBO Journal* 39, no. 24 (2020): e104948.

114. P. Szalai, L. K. Hagen, F. Sætre, et al., "Autophagic Bulk Sequestration of Cytosolic Cargo Is Independent of LC3, But Requires GABARAPs," *Experimental Cell Research* 333, no. 1 (2015): 21–38.

115. N. Mizushima and L. O. Murphy, "Autophagy Assays for Biological Discovery and Therapeutic Development," *Trends in Biochemical Sciences* 45, no. 12 (2020): 1080–1093.

116. A. Kuma, M. Matsui, and N. Mizushima, "LC3, an Autophagosome Marker, Can Be Incorporated Into Protein Aggregates Independent of Autophagy: Caution in the Interpretation of LC3 Localization," *Autophagy* 3, no. 4 (2007): 323–328.

117. G. Runwal, E. Stamatakou, F. H. Siddiqi, C. Puri, Y. Zhu, and D. C. Rubinsztein, "LC3-Positive Structures Are Prominent in Autophagy-Deficient Cells," *Scientific Reports* 9, no. 1 (2019): 1–14.

118. E. Turco, A. Savova, F. Gere, et al., "Reconstitution Defines the Roles of p62, NBR1 and TAX1BP1 in Ubiquitin Condensate Formation and Autophagy Initiation," *Nature Communications* 12, no. 1 (2021): 5212.

119. A. Khaminets, T. Heinrich, M. Mari, et al., "Regulation of Endoplasmic Reticulum Turnover by Selective Autophagy," *Nature* 522, no. 7556 (2015): 354–358.

120. T. Murakawa, O. Yamaguchi, A. Hashimoto, et al., "Bcl-2-Like Protein 13 Is a Mammalian Atg32 Homologue That Mediates Mitophagy and Mitochondrial Fragmentation," *Nature Communications* 6, no. 1 (2015): 7527.

121. C. Kumsta, J. T. Chang, R. Lee, et al., "The Autophagy Receptor p62/SQST-1 Promotes Proteostasis and Longevity in *C. elegans* by Inducing Autophagy," *Nature Communications* 10, no. 1 (2019): 5648.

122. A. Reggio, V. Buonomo, R. Berkane, et al., "Role of FAM134 Paralogues in Endoplasmic Reticulum Remodeling, ER-Phagy, and Collagen Quality Control," *EMBO Reports* 22, no. 9 (2021): e52289.

123. T. P. Ashford and K. R. Porter, "Cytoplasmic Components in Hepatic Cell Lysosomes," *Journal of Cell Biology* 12, no. 1 (1962): 198–202.

124. S. L. Clark, Jr., "Cellular Differentiation in the Kidneys of Newborn Mice studies With the Electron Microscope," *Journal of Biophysical and Biochemical Cytology* 3, no. 3 (1957): 349–362.

125. A. B. Novikoff, "The Proximal Tubule Cell in Experimental Hydronephrosis," *Journal of Biophysical and Biochemical Cytology* 6, no. 1 (1959): 136–138.

126. C. de Duve, "The Lysosome," *Scientific American* 208 (1963): 64–72.

127. Z. Hruban, R. G. Kleinfeld, B. Spargo, R. W. Wissler, and H. Swift, "Focal Cytoplasmic Degradation," *American Journal of Pathology* 42, no. 6 (1963): 657–683.

128. A. B. Novikoff, E. Essner, and N. Quintana, "Golgi Apparatus and Lysosomes," *Federation Proceedings* 23 (1964): 1010–1022.

129. M. Locke and J. V. Collins, "The Structure and Formation of Protein Granules in the Fat Body of an Insect," *Journal of Cell Biology* 26, no. 3 (1965): 857–884.

130. H. F. Kern and D. Kern, "Electron Microscopic studies on the Action of Cobalt Chloride on the Exocrine Pancreatic Tissue in Guinea Pigs," *Virchows Archiv B: Cell Pathology* 4, no. 1 (1969): 54–70.

131. T. Noda and M. G. Farquhar, "A Non-Autophagic Pathway for Diversion of ER Secretory Proteins to Lysosomes," *Journal of Cell Biology* 119, no. 1 (1992): 85–97.

132. J. Tooze, M. Hollinshead, T. Ludwig, K. Howell, B. Hoflack, and H. Kern, "In Exocrine Pancreas, the Basolateral Endocytic Pathway Converges With the Autophagic Pathway Immediately After the Early Endosome," *Journal of Cell Biology* 111, no. 2 (1990): 329–345.

16000854, 2024, 10, Downloaded from https://onlinelibrary.wiley.com/doi/10.1111/tra.12957 by Biblioteca universitaria di Lugano, Wiley Online Library on [18/11/2024]. See the Terms and Conditions (https://onlinelibrary.wiley.com/terms-and-conditions) on Wiley Online Library for rules of use; OA articles are governed by the applicable Creative Commons License

133. R. P. Bolender and E. R. Weibel, "A Morphometric Study of the Removal of Phenobarbital-Induced Membranes From Hepatocytes After Cessation of Treatment," *Journal of Cell Biology* 56, no. 3 (1973): 746–761.

134. H. An, A. Ordureau, J. A. Paulo, C. J. Shoemaker, V. Denic, and J. W. Harper, "TEX264 Is an Endoplasmic Reticulum-Resident ATG8-Interacting Protein Critical for ER Remodeling During Nutrient Stress," *Molecular Cell* 74, no. 5 (2019): 891–908.e810.

135. M. J. Hoyer, C. Capitanio, I. R. Smith, et al., "Combinatorial Selective ER-Phagy Remodels the ER During Neurogenesis," *Nature Cell Biology* 26, no. 3 (2024): 378–392.

136. Y. Hirota, S.-I. Yamashita, Y. Kurihara, et al., "Mitophagy Is Primarily Due to Alternative Autophagy and Requires the MAPK1 and MAPK14 Signaling Pathways," *Autophagy* 11, no. 2 (2015): 332–343.

137. T. Kogure, H. Kawano, Y. Abe, and A. Miyawaki, "Fluorescence Imaging Using a Fluorescent Protein With a Large Stokes Shift," *Methods* 45, no. 3 (2008): 223–226.

138. N. Sun, J. Yun, J. Liu, et al., "Measuring in Vivo Mitophagy," *Molecular Cell* 60, no. 4 (2015): 685–696.

139. N. Sun, D. Malide, J. Liu, I. I. Rovira, C. A. Combs, and T. Finkel, "A Fluorescence-Based Imaging Method to Measure In Vitro and In Vivo Mitophagy Using Mt-Keima," *Nature Protocols* 12, no. 8 (2017): 1576–1587.

140. K. L. Hickey, S. Swarup, I. R. Smith, et al., "Proteome Census Upon Nutrient Stress Reveals Golgiphagy Membrane Receptors," *Nature* 623, no. 7985 (2023): 167–174.

141. J. R. Liang, E. Lingeman, T. Luong, et al., "A Genome-Wide ER-Phagy Screen Highlights Key Roles of Mitochondrial Metabolism and ER-Resident UFMylation," *Cell* 180 (2020): 1160–1177.

142. L. Cinque, C. De Leonibus, M. Iavazzo, et al., "MiT/TFE Factors Control ER-Phagy via Transcriptional Regulation of FAM134B," *EMBO Journal* 39, no. 17 (2020): e105696.

143. F. Fumagalli, J. Noack, T. J. Bergmann, et al., "Translocon Component Sec62 Acts in Endoplasmic Reticulum Turnover During Stress Recovery," *Nature Cell Biology* 18, no. 11 (2016): 1173–1184.

144. M. Loi, A. Raimondi, D. Morone, and M. Molinari, "ESCRT-III-Driven Piecemeal Micro-ER-Phagy Remodels the ER During Recovery From ER Stress," *Nature Communications* 10, no. 1 (2019): 5058.

145. I. Fregno and M. Molinari, "Proteasomal and Lysosomal Clearance of Faulty Secretory Proteins: ER-Associated Degradation (ERAD) and ER-to-Lysosome-Associated Degradation (ERLAD) Pathways," *Critical Reviews in Biochemistry and Molecular Biology* 54, no. 2 (2019): 153–163.

146. I. Fregno, E. Fasana, T. Solda, C. Galli, and M. Molinari, "N-Glycan Processing Selects ERAD-Resistant Misfolded Proteins for ER-to-Lysosome-Associated Degradation," *EMBO Journal* 40, no. 15 (2021): e107240.

147. T. Cremer, L. M. Voortman, E. Bos, et al., "RNF26 Binds Perinuclear Vimentin Filaments to Integrate ER and Endolysosomal Responses to Proteotoxic Stress," *EMBO Journal* 42, no. 18 (2023): e111252.

148. E. Fasana, I. Fregno, C. Galli, T. Soldà, and M. Molinari, "ER-to-Lysosome-Associated Degradation Acts as Failsafe Mechanism Upon ERAD Dysfunction," *EMBO Reports* 25, no. 6 (2024): 2773–2785.

149. S. Martens, I. Parvanova, J. Zerrahn, et al., "Disruption of Toxoplasma Gondii Parasitophorous Vacuoles by the Mouse p47-Resistance GTPases," *PLoS Pathogens* 1, no. 3 (2005): e24.

150. P. A. Beare, D. Howe, D. C. Cockrell, A. Omsland, B. Hansen, and R. A. Heinzen, "Characterization of a Coxiella Burnetii ftsZ Mutant Generated by Himar1 Transposon Mutagenesis," *Journal of Bacteriology* 191, no. 5 (2009): 1369–1381.

151. I. Fregno and M. Molinari, "Endoplasmic Reticulum Turnover: ER-Phagy and Other Flavors in Selective and Non-Selective ER Clearance," *F1000Research* 7 (2018): 454.

152. M. Rudinskiy and M. Molinari, "ER-To-Lysosome-Associated Degradation in a Nutshell: Mammalian, Yeast, and Plant ER-Phagy as Induced by Misfolded Proteins," *FEBS Letters* 597, no. 15 (2023): 1928–1945.

153. J. H. Teckman and D. H. Perlmutter, "Retention of Mutant Alpha(1)-Antitrypsin Z in Endoplasmic Reticulum Is Associated With an Autophagic Response," *American Journal of Physiology. Gastrointestinal and Liver Physiology* 279, no. 5 (2000): G961–G974.

154. T. Kamimoto, S. Shoji, T. Hidvegi, et al., "Intracellular Inclusions Containing Mutant Alpha1-Antitrypsin Z Are Propagated in the Absence of Autophagic Activity," *Journal of Biological Chemistry* 281, no. 7 (2006): 4467–4476.

155. H. Kroeger, E. Miranda, I. MacLeod, et al., "Endoplasmic Reticulum-Associated Degradation (ERAD) and Autophagy Cooperate to Degrade Polymerogenic Mutant Serpins," *Journal of Biological Chemistry* 284, no. 34 (2009): 22793–22802.

156. E. Miranda, J. Perez, U. I. Ekeowa, et al., "A Novel Monoclonal Antibody to Characterize Pathogenic Polymers in Liver Disease Associated With Alpha(1)-Antitrypsin Deficiency," *Hepatology* 52, no. 3 (2010): 1078–1088.

157. P. Strnad, N. G. McElvaney, and D. A. Lomas, "Alpha1-Antitrypsin Deficiency," *New England Journal of Medicine* 382, no. 15 (2020): 1443–1455.

158. K. B. Kruse, J. L. Brodsky, and A. A. McCracken, "Characterization of an ERAD Gene as VPS30/ATG6 Reveals Two Alternative and Functionally Distinct Protein Quality Control Pathways: One for Soluble Z Variant of Human Alpha-1 Proteinase Inhibitor (A1PiZ) and Another for Aggregates of A1PiZ," *Molecular Biology of the Cell* 17, no. 1 (2006): 203–212.

159. Y. Cui, S. Parashar, M. Zahoor, et al., "A COPII Subunit Acts With an Autophagy Receptor to Target Endoplasmic Reticulum for Degradation," *Science* 365, no. 6448 (2019): 53–60.

160. C. L. Gelling, I. W. Dawes, D. H. Perlmutter, E. A. Fisher, and J. L. Brodsky, "The Endosomal Protein-Sorting Receptor Sortilin Has a Role in Trafficking Alpha-1 Antitrypsin," *Genetics* 192, no. 3 (2012): 889–903.

161. A. Forrester, C. De Leonibus, P. Grumati, et al., "A Selective ER-Phagy Exerts Procollagen Quality Control via a Calnexin-FAM134B Complex," *EMBO Journal* 38, no. 2 (2019): e99847.

162. C. De Leonibus, M. Maddaluno, R. Ferriero, et al., "Sestrin2 Drives ER-Phagy in Response to Protein Misfolding," *Developmental Cell* S1534-5807, no. 24 (2024): 441–446.

163. S. Ishii, H. Chino, K. L. Ode, et al., "CCPG1 Recognizes ER Luminal Proteins for Selective ER-Phagy," *Molecular Biology of the Cell* 34, no. 4 (2023): ar29.

164. A. Tomihari, M. Kiyota, A. Matsuura, and E. Itakura, "Alpha 2-Macroglobulin Acts as a Clearance Factor in the Lysosomal Degradation of Extracellular Misfolded Proteins," *Scientific Reports* 13, no. 1 (2023): 4680.

165. E. Itakura, M. Chiba, T. Murata, and A. Matsuura, "Heparan Sulfate Is a Clearance Receptor for Aberrant Extracellular Proteins," *Journal of Cell Biology* 219, no. 3 (2020): e201911126.

166. I. Ron and M. Horowitz, "ER Retention and Degradation as the Molecular Basis Underlying Gaucher Disease Heterogeneity," *Human Molecular Genetics* 14, no. 16 (2005): 2387–2398.

167. C. Xu, N. Sakai, M. Taniike, K. Inui, and K. Ozono, "Six Novel Mutations Detected in the GALC Gene in 17 Japanese Patients With Krabbe Disease, and New Genotype-Phenotype Correlation," *Journal of Human Genetics* 51, no. 6 (2006): 548–554.

16000854, 2024, 10, Downloaded from https://onlinelibrary.wiley.com/doi/10.1111/tra.12957 by Biblioteca universitaria di Lugano, Wiley Online Library on [18/11/2024]. See the Terms and Conditions (https://onlinelibrary.wiley.com/terms-and-conditions) on Wiley Online Library for rules of use; OA articles are governed by the applicable Creative Commons License

168. M. A. Hossain, T. Otomo, S. Saito, et al., "Late-Onset Krabbe Disease Is Predominant in Japan and Its Mutant Precursor Protein Undergoes More Effective Processing Than the Infantile-Onset Form," *Gene* 534, no. 2 (2014): 144–154.

169. R. L. Lieberman, J. A. D'Aquino, D. Ringe, and G. A. Petsko, "Effects of pH and Iminosugar Pharmacological Chaperones on Lysosomal Glycosidase Structure and Stability," *Biochemistry* 48, no. 22 (2009): 4816–4827.

170. A. Kato, Y. Yamashita, S. Nakagawa, et al., "2,5-Dideoxy-2,5-I mino-D-Altritol as a New Class of Pharmacological Chaperone for Fabry Disease," *Bioorganic & Medicinal Chemistry* 18, no. 11 (2010): 3790–3794.

171. M. Morita, S. Saito, K. Ikeda, et al., "Structural Bases of GM1 Gangliosidosis and Morquio B Disease," *Journal of Human Genetics* 54, no. 9 (2009): 510–515.

172. I. S. Abumansour, N. Yuskiv, E. Paschke, and S. Stockler-Ipsiroglu, "Morquio-B Disease: Clinical and Genetic Characteristics of a Distinct GLB1-Related Dysostosis Multiplex," *JIMD Reports* 51, no. 1 (2020): 30–44.

173. S. Y. Cho and D.-K. Jin, "GLB1-Related Disorders: GM1 Gangliosidosis and Morquio B Disease," *Journal of Gene Medicine* 18, no. 1 (2021): 16–23.

174. M. Bhat, A. Nambiar, L. Edakkandiyil, et al., "A Genetically-Encoded Fluorescence-Based Reporter to Spatiotemporally Investigate Mannose-6-Phosphate Pathway," *Molecular Biology of the Cell* 35, no. 8 (2024): mr6.

175. S. Ishii, A. Matsuura, and E. Itakura, "Identification of a Factor Controlling Lysosomal Homeostasis Using a Novel Lysosomal Trafficking Probe," *Scientific Reports* 9, no. 1 (2019): 11635.

176. C. A. Hubner and I. Dikic, "ER-Phagy and Human Diseases," *Cell Death and Differentiation* 27, no. 3 (2020): 833–842.

177. M. Molinari, "ER-Phagy Responses in Yeast, Plants, and Mammalian Cells and Their Crosstalk With UPR and ERAD," *Developmental Cell* 56, no. 7 (2021): 949–966.

178. J. R. Liang and J. E. Corn, "A CRISPR View on Autophagy," *Trends in Cell Biology* 32, no. 12 (2022): 1008–1022.

179. T. G. McWilliams, A. R. Prescott, G. F. G. Allen, et al., "Mito-QC Illuminates Mitophagy and Mitochondrial Architecture In Vivo," *Journal of Cell Biology* 214, no. 3 (2016): 333–345.

180. T. G. McWilliams, A. R. Prescott, L. Montava-Garriga, et al., "Basal Mitophagy Occurs Independently of PINK1 in Mouse Tissues of High Metabolic Demand," *Cell Metabolism* 27, no. 2 (2018): 439–449 e435.

181. S. Aoyama, Y. Nishida, H. Uzawa, et al., "Monitoring Autophagic Flux In Vivo Revealed Its Physiological Response and Significance of Heterogeneity in Pancreatic Beta Cells," *Cell Chemical Biology* 30, no. 6 (2023): 658–671.e654.

182. G. Di Lorenzo, F. Iavarone, M. Maddaluno, et al., "Phosphorylation of FAM134C by CK2 Controls Starvation-Induced ER-Phagy," *Science Advances* 8, no. 35 (2022): eabo1215.

183. J. W. Lichtman and J. A. Conchello, "Fluorescence Microscopy," *Nature Methods* 2, no. 12 (2005): 910–919.

184. H. Balasubramanian, C. M. Hobson, T.-L. Chew, and J. S. Aaron, "Imagining the Future of Optical Microscopy: Everything, Everywhere, All at Once," *Communications Biology* 6, no. 1 (2023): 1096.

185. M. K. Kucińska, J. Fedry, C. Galli, et al., "TMX4-Driven LINC Complex Disassembly and Asymmetric Autophagy of the Nuclear Envelope Upon Acute ER Stress," *Nature Communications* 14, no. 1 (2023): 3497.

186. J. Jonkman, C. M. Brown, G. D. Wright, K. I. Anderson, and A. J. North, "Tutorial: Guidance for Quantitative Confocal Microscopy," *Nature Protocols* 15, no. 5 (2020): 1585–1611.

187. M. S. Frei, M. Tarnawski, M. J. Roberti, B. Koch, J. Hiblot, and K. Johnsson, "Engineered HaloTag Variants for Fluorescence Lifetime Multiplexing," *Nature Methods* 19, no. 1 (2022): 65–70.

188. A. Keppler, S. Gendreizig, T. Gronemeyer, H. Pick, H. Vogel, and K. Johnsson, "A General Method for the Covalent Labeling of Fusion Proteins With Small Molecules In Vivo," *Nature Biotechnology* 21, no. 1 (2003): 86–89.

189. R. Dreyer, R. Pfukwa, S. Barth, R. Hunter, and B. Klumperman, "The Evolution of SNAP-Tag Labels," *Biomacromolecules* 24, no. 2 (2023): 517–530.

190. A. Gautier, A. Juillerat, C. Heinis, et al., "An Engineered Protein Tag for Multiprotein Labeling in Living Cells," *Chemistry & Biology* 15, no. 2 (2008): 128–136.

191. J. Oreopoulos, R. Berman, and M. Browne, "Spinning-Disk Confocal Microscopy: Present Technology and Future Trends," *Methods in Cell Biology* 123 (2014): 153–175.

192. B. T. Bajar, A. J. Lam, R. K. Badiee, et al., "Fluorescent Indicators for Simultaneous Reporting of all Four Cell Cycle Phases," *Nature Methods* 13, no. 12 (2016): 993–996.

193. K. Thorn, "Chapter 23—Spinning-Disk Confocal Microscopy of Yeast," *Methods in Enzymology*, 470 (2010), 581–602.

194. L. Schermelleh, A. Ferrand, T. Huser, et al., "Super-Resolution Microscopy Demystified," *Nature Cell Biology* 21, no. 1 (2019): 72–84.

195. K. Prakash, B. Diederich, R. Heintzmann, and L. Schermelleh, "Super-Resolution Microscopy: A Brief History and New Avenues," *Philosophical Transactions of the Royal Society A – Mathematical Physical and Engineering Sciences* 380, no. 2220 (2022): 20210110.

196. S. J. Sahl, S. W. Hell, and S. Jakobs, "Fluorescence Nanoscopy in Cell Biology," *Nature Reviews. Molecular Cell Biology* 18, no. 11 (2017): 685–701.

197. M. Lelek, M. T. Gyparaki, G. Beliu, et al., "Single-Molecule Localization Microscopy," *Nature Reviews Methods Primers* 1, no. 1 (2021): 1–60.

198. S. W. Hell, "Far-Field Optical Nanoscopy," *Science* 316, no. 5828 (2007): 1153–1158.

199. M. Hofmann, C. Eggeling, S. Jakobs, and S. W. Hell, "Breaking the Diffraction Barrier in Fluorescence Microscopy at Low Light Intensities by Using Reversibly Photoswitchable Proteins," *National Academy of Sciences of the United States of America* 102, no. 49 (2005): 17565–17569.

200. F. Balzarotti, Y. Eilers, K. C. Gwosch, et al., "Nanometer Resolution Imaging and Tracking of Fluorescent Molecules With Minimal Photon Fluxes," *Science* 355, no. 6325 (2017): 606–612.

201. Y. Eilers, H. Ta, K. C. Gwosch, F. Balzarotti, and S. W. Hell, "MINFLUX Monitors Rapid Molecular Jumps With Superior Spatiotemporal Resolution," *National Academy of Sciences of the United States of America* 115, no. 24 (2018): 6117–6122.

202. M. Weber, M. Leutenegger, S. Stoldt, et al., "MINSTED Fluorescence Localization and Nanoscopy," *Nature Photonics* 15, no. 5 (2021): 361–366.

203. L. Scheiderer, H. Von Der Emde, M. Hesselink, M. Weber, and S. W. Hell, "MINSTED Tracking of Single Biomolecules," *Nature Methods* 21, no. 4 (2024): 569–573.

204. C. Banerjee, D. Mehra, D. Song, et al., "ULK1 Forms Distinct Oligomeric States and Nanoscopic Structures During Autophagy Initiation," *Science Advances* 9, no. 39 (2023): eadh4094.

16000854, 2024, 10, Downloaded from https://onlinelibrary.wiley.com/doi/10.1111/tra.12957 by Biblioteca universitaria di Lugano, Wiley Online Library on [18/11/2024]. See the Terms and Conditions (https://onlinelibrary.wiley.com/terms-and-conditions) on Wiley Online Library for rules of use; OA articles are governed by the applicable Creative Commons License

205. C. Banerjee, E. M. Puchner, and D. H. Kim, "ULK1 Seen at the Single-Molecule Level During Autophagy Initiation," *Autophagy* 20, no. 3 (2024): 707–708.

206. A. T. Wassie, Y. Zhao, and E. S. Boyden, "Expansion Microscopy: Principles and Uses in Biological Research," *Nature Methods* 16, no. 1 (2019): 33–41.

207. M. H. Laporte, N. Klena, V. Hamel, and P. Guichard, "Visualizing the Native Cellular Organization by Coupling Cryofixation With Expansion Microscopy (Cryo-ExM)," *Nature Methods* 19, no. 2 (2022): 216–222.

208. A. P. Cuny, F. P. Schlottmann, J. C. Ewald, S. Pelet, and K. M. Schmoller, "Live Cell Microscopy: From Image to Insight," *Biophysics Reviews (Melville)* 3, no. 2 (2022): 021302.

209. P. Dalle Pezze, E. Karanasios, V. Kandia, et al., "ATG13 Dynamics in Nonselective Autophagy and Mitophagy: Insights From Live Imaging studies and Mathematical Modeling," *Autophagy* 17, no. 5 (2021): 1131–1141.

210. A. Du Toit, J.-H. S. Hofmeyr, T. J. Gniadek, and B. Loos, "Measuring Autophagosome Flux," *Autophagy* 14, no. 6 (2018): 1060–1071.

211. S. Ghosh, T. A. Dellibovi-Ragheb, A. Kerviel, et al., "β-Coronaviruses Use Lysosomes for Egress Instead of the Biosynthetic Secretory Pathway," *Cell* 183, no. 6 (2020): 1520–1535.e1514.

212. B.-C. Chen, W. R. Legant, K. Wang, et al., "Lattice Light-Sheet Microscopy: Imaging Molecules to Embryos at High Spatiotemporal Resolution," *Science* 346, no. 6208 (2014): 1257998.

213. Y. C. Tsai, W. C. Tang, C. S. L. Low, et al., "Rapid High Resolution 3D Imaging of Expanded Biological Specimens With Lattice Light Sheet Microscopy," *Methods* 174 (2020): 11–19.

214. M. G. L. Gustafsson, "Surpassing the Lateral Resolution Limit by a Factor of Two Using Structured Illumination Microscopy," *Journal of Microscopy* 198, no. 2 (2000): 82–87.

215. M. Saxena, G. Eluru, and S. S. Gorthi, "Structured Illumination Microscopy," *Advances in Optics and Photonics* 7, no. 2 (2015): 241.

216. F. Ströhl and C. F. Kaminski, "Frontiers in Structured Illumination Microscopy," *Optica* 3, no. 6 (2016): 667.

217. Y. Ma, K. Wen, M. Liu, et al., "Recent Advances in Structured Illumination Microscopy," *Journal of Physics: Photonics* 3, no. 2 (2021): 024009.

218. Z. Man, H. Cui, Z. Lv, et al., "Organic Nanoparticles-Assisted Low-Power STED Nanoscopy," *Nano Letters* 21, no. 8 (2021): 3487–3494.

219. J. O. Wirth, L. Scheiderer, T. Engelhardt, J. Engelhardt, J. Matthias, and S. W. Hell, "MINFLUX Dissects the Unimpeded Walking of Kinesin-1," *Science* 379, no. 6636 (2023): 1004–1010.

220. M. Castello, G. Tortarolo, M. Buttafava, et al., "A Robust and Versatile Platform for Image Scanning Microscopy Enabling Super-Resolution FLIM," *Nature Methods* 16, no. 2 (2019): 175–178.

221. R. Datta, T. M. Heaster, J. T. Sharick, A. A. Gillette, and M. C. Skala, "Fluorescence Lifetime Imaging Microscopy: Fundamentals and Advances in Instrumentation, Analysis, and Applications," *Journal of Biomedical Optics* 25, no. 7 (2020): 1.

222. E. B. Gökerküçük, A. Cheron, M. Tramier, and G. Bertolin, "The LC3B FRET Biosensor Monitors the Modes of Action of ATG4B During Autophagy in Living Cells," *Autophagy* 19, no. 8 (2023): 2275–2295.

223. A. Ahmed, J. Schoberer, E. Cooke, and S. W. Botchway, "Multicolor FRET-FLIM Microscopy to Analyze Multiprotein Interactions in Live Cells," in *Methods in Molecular Biology* (US: Springer US, 2021), 287–301.

224. B. Guan, Y.-T. Jiang, D.-L. Lin, W.-H. Lin, and H.-W. Xue, "Phosphatidic Acid Suppresses Autophagy Through Competitive Inhibition by Binding GAPC (Glyceraldehyde-3-Phosphate Dehydrogenase) and PGK (Phosphoglycerate Kinase) Proteins," *Autophagy* 18, no. 11 (2022): 2656–2670.

225. R. S. Saleeb, D. M. Kavanagh, A. R. Dun, P. A. Dalgarno, and R. R. Duncan, "A VPS33A-Binding Motif on Syntaxin 17 Controls Autophagy Completion in Mammalian Cells," *Journal of Biological Chemistry* 294, no. 11 (2019): 4188–4201.

226. E.-L. Eskelinen, F. Reggiori, M. Baba, A. L. Kovács, and P. O. Seglen, "Seeing Is Believing: The Impact of Electron Microscopy on Autophagy Research," *Autophagy* 7, no. 9 (2011): 935–956.

227. J. Rhodin, *Correlation of Ultrastructural Organization and Function in Normal and Experimentally Changed Proximal Tubule Cells of the Mouse Kidney* (Stockholm, Sweden: Dept. of Anatomy, Karolinska Institutet, 1954).

228. M. U. Hutchins, M. Veenhuis, and D. J. Klionsky, "Peroxisome Degradation in *Saccharomyces cerevisiae* Is Dependent on Machinery of Macroautophagy and the Cvt Pathway," *Journal of Cell Science* 112, no. 22 (1999): 4079–4087.

229. M. K. Higgins and H. T. McMahon, "Snap-Shots of Clathrin-Mediated Endocytosis," *Trends in Biochemical Sciences* 27, no. 5 (2002): 257–263.

230. R. Singh, S. Kaushik, Y. Wang, et al., "Autophagy Regulates Lipid Metabolism," *Nature* 458, no. 7242 (2009): 1131–1135.

231. L. Graham and J. M. Orenstein, "Processing Tissue and Cells for Transmission Electron Microscopy in Diagnostic Pathology and Research," *Nature Protocols* 2, no. 10 (2007): 2439–2450.

232. L. Gan and G. J. Jensen, "Electron Tomography of Cells," *Quarterly Reviews of Biophysics* 45, no. 1 (2012): 27–56.

233. T. M. Mayhew, J. M. Lucocq, and G. Griffiths, "Relative Labelling Index: A Novel Stereological Approach to Test for Non-Random Immunogold Labelling of Organelles and Membranes on Transmission Electron Microscopy Thin Sections," *Journal of Microscopy* 205, no. 2 (2002): 153–164.

234. T. M. Mayhew, "Quantitative Immunoelectron Microscopy," *Methods in Molecular Biology* 369(2007), 309–329.

235. A. De Mazière, J. Van Der Beek, S. Van Dijk, et al., "An Optimized Protocol for Immuno-Electron Microscopy of Endogenous LC3," *Autophagy* 18, no. 12 (2022): 3004–3022.

236. L. M. Collinson, C. Bosch, A. Bullen, et al., "Volume EM: A Quiet Revolution Takes Shape," *Nature Methods* 20, no. 6 (2023): 777–782.

237. C. J. Peddie, C. Genoud, A. Kreshuk, et al., "Volume Electron Microscopy," *Nature Reviews Methods Primers* 2 (2022): 51.

238. Y. C. Liao, S. Pang, W. P. Li, et al., "COPII With ALG2 and ESCRTs Control Lysosome-Dependent Microautophagy of ER Exit Sites," *Developmental Cell* 59, no. 11 (2024): 1410–1424.

239. E.-L. Eskelinen, "To Be or Not to Be? Examples of Incorrect Identification of Autophagic Compartments in Conventional Transmission Electron Microscopy of Mammalian Cells," *Autophagy* 4, no. 2 (2008): 257–260.

240. K. Van Den Dries, J. Fransen, and A. Cambi, "Fluorescence CLEM in Biology: Historic Developments and Current Super-Resolution Applications," *FEBS Letters* 596, no. 19 (2022): 2486–2496.

241. K. A. Taylor and R. M. Glaeser, "Electron Diffraction of Frozen, Hydrated Protein Crystals," *Science* 186, no. 4168 (1974): 1036–1037.

242. J. Dubochet, M. Adrian, J. J. Chang, et al., "Cryo-Electron Microscopy of Vitrified Specimens," *Quarterly Reviews of Biophysics* 21, no. 2 (1988): 129–228.

243. E. Nogales and J. Mahamid, "Bridging Structural and Cell Biology With Cryo-Electron Microscopy," *Nature* 628, no. 8006 (2024): 47–56.

16000854, 2024, 10, Downloaded from https://onlinelibrary.wiley.com/doi/10.1111/tra.12957 by Biblioteca universitaria di Lugano, Wiley Online Library on [18/11/2024]. See the Terms and Conditions (https://onlinelibrary.wiley.com/terms-and-conditions) on Wiley Online Library for rules of use; OA articles are governed by the applicable Creative Commons License

244. T. Nakane, A. Kotecha, A. Sente, et al., "Single-Particle Cryo-EM at Atomic Resolution," *Nature* 587, no. 7832 (2020): 152–156.

245. K. M. Yip, N. Fischer, E. Paknia, A. Chari, and H. Stark, "Atomic-Resolution Protein Structure Determination by Cryo-EM," *Nature* 587, no. 7832 (2020): 157–161.

246. S. Baskaran, L. A. Carlson, G. Stjepanovic, et al., "Architecture and Dynamics of the Autophagic Phosphatidylinositol 3-Kinase Complex," *eLife* 3 (2014): e05115.

247. A. Rigort, F. J. Bäuerlein, E. Villa, et al., "Focused Ion Beam Micromachining of Eukaryotic Cells for Cryoelectron Tomography," *Proceedings of the National Academy of Sciences of the United States of America* 109, no. 12 (2012): 4449–4454.

248. C. Berger, M. Dumoux, T. Glen, et al., "Plasma FIB Milling for the Determination of Structures In Situ," *Nature Communications* 14, no. 1 (2023): 629.

249. A. Bieber, C. Capitanio, P. S. Erdmann, et al., "In Situ Structural Analysis Reveals Membrane Shape Transitions During Autophagosome Formation," *National Academy of Sciences of the United States of America* 119, no. 39 (2022): e2209823119.

250. M. Turk and W. Baumeister, "The Promise and the Challenges of Cryo-Electron Tomography," *FEBS Letters* 594, no. 20 (2020): 3243–3261.

251. M. Molinari, "ER Remodelling by ER-Phagy in Neurogenesis," *Nature Cell Biology* 26, no. 3 (2024): 316–317.

252. J. Miné-Hattab, "When Fixation Creates Fiction," *eLife* 12 (2023): e85671.

253. S. Irgen-Gioro, S. Yoshida, V. Walling, and S. Chong, "Fixation Can Change the Appearance of Phase Separation in Living Cells," *eLife* 11 (2022): e79903.

254. M. A. Phillips, M. Harkiolaki, D. M. Susano Pinto, et al., "CryoSIM: Super-Resolution 3D Structured Illumination Cryogenic Fluorescence Microscopy for Correlated Ultrastructural Imaging," *Optica* 7, no. 7 (2020): 802–812.

255. M. W. Tuijtel, A. J. Koster, S. Jakobs, F. G. A. Faas, and T. H. Sharp, "Correlative Cryo Super-Resolution Light and Electron Microscopy on Mammalian Cells Using Fluorescent Proteins," *Scientific Reports* 9, no. 1 (2019): 1369.

256. U. Boehm, G. Nelson, C. M. Brown, et al., "QUAREP-LiMi: A Community Endeavor to Advance Quality Assessment and Reproducibility in Light Microscopy," *Nature Methods* 18, no. 12 (2021): 1423–1426.

257. L. Fan, F. Zhang, H. Fan, and C. Zhang, "Brief Review of Image Denoising Techniques," *Visual Computing for Industry, Biomedicine, and Art* 2, no. 1 (2019): 7.

258. I. Gómez-Conde, S. S. Caetano, C. E. Tadokoro, and D. N. Olivieri, "Stabilizing 3D In Vivo Intravital Microscopy Images With an Iteratively Refined Soft-Tissue Model for Immunology Experiments," *Computers in Biology and Medicine* 64 (2015): 246–260.

259. C. W. Wang, S. M. Ka, and A. Chen, "Robust Image Registration of Biological Microscopic Images," *Scientific Reports* 4 (2014): 6050.

260. H. R. Boveiri, R. Khayami, R. Javidan, and A. Mehdizadeh, "Medical Image Registration Using Deep Neural Networks: A Comprehensive Review," *Computers and Electrical Engineering* 87 (2020): 106767.

261. J. R. Swedlow, "Quantitative Fluorescence Microscopy and Image Deconvolution," *Methods in Cell Biology* 114 (2013): 407–426.

262. K. Jaqaman, D. Loerke, M. Mettlen, et al., "Robust Single-Particle Tracking in Live-Cell Time-Lapse Sequences," *Nature Methods* 5, no. 8 (2008): 695–702.

263. J. Y. Tinevez, N. Perry, J. Schindelin, et al., "TrackMate: An Open and Extensible Platform for Single-Particle Tracking," *Methods* 115 (2017): 80–90.

264. A. Zweifach, "Determining How Many Cells to Average for Statistical Testing of Microscopy Experiments," *Journal of Cell Biology* 223, no. 8 (2024): e202401074.

265. C. Belthangady and L. A. Royer, "Applications, Promises, and Pitfalls of Deep Learning for Fluorescence Image Reconstruction," *Nature Methods* 16, no. 12 (2019): 1215–1225.

266. J. G. Greener, S. M. Kandathil, L. Moffat, and D. T. Jones, "A Guide to Machine Learning for Biologists," *Nature Reviews. Molecular Cell Biology* 23, no. 1 (2022): 40–55.

267. Y. LeCun, Y. Bengio, and G. Hinton, "Deep Learning," *Nature* 521, no. 7553 (2015): 436–444.

268. D. C. Barral, L. Staiano, C. Guimas Almeida, et al., "Current Methods to Analyze Lysosome Morphology, Positioning, Motility and Function," *Traffic* 23, no. 5 (2022): 238–269.

269. T. Falk, D. Mai, R. Bensch, et al., "U-Net: Deep Learning for Cell Counting, Detection, and Morphometry," *Nature Methods* 16, no. 1 (2019): 67–70.

270. V. Badrinarayanan, A. Kendall, and R. Cipolla, "SegNet: A Deep Convolutional Encoder-Decoder Architecture for Image Segmentation," *IEEE Transactions on Pattern Analysis and Machine Intelligence* 39, no. 12 (2017): 2481–2495.

271. L. Jin, B. Liu, F. Zhao, et al., "Deep Learning Enables Structured Illumination Microscopy With Low Light Levels and Enhanced Speed," *Nature Communications* 11, no. 1 (2020): 1934.

272. C. M. Pate, J. L. Hart, and M. L. Taheri, "RapidEELS: Machine Learning for Denoising and Classification in Rapid Acquisition Electron Energy Loss Spectroscopy," *Scientific Reports* 11, no. 1 (2021): 19515.

273. P. Wijesinghe and K. Dholakia, "Emergent Physics-Informed Design of Deep Learning for Microscopy," *Journal of Physics: Photonics* 3, no. 2 (2021): 021003.

274. M. Weigert, U. Schmidt, T. Boothe, et al., "Content-Aware Image Restoration: Pushing the Limits of Fluorescence Microscopy," *Nature Methods* 15, no. 12 (2018): 1090–1097.

275. C. N. Christensen, E. N. Ward, M. Lu, P. Lio, and C. F. Kaminski, "ML-SIM: Universal Reconstruction of Structured Illumination Microscopy Images Using Transfer Learning," *Biomedical Optics Express* 12, no. 5 (2021): 2720–2733.

276. X. Chong, M. Cheng, W. Fan, Q. Li, and H. Leung, "M-Denoiser: Unsupervised Image Denoising for Real-World Optical and Electron Microscopy Data," *Computers in Biology and Medicine* 164 (2023): 107308.

277. P. Wijesinghe, S. Corsetti, D. J. X. Chow, S. Sakata, K. R. Dunning, and K. Dholakia, "Experimentally Unsupervised Deconvolution for Light-Sheet Microscopy With Propagation-Invariant Beams," *Light: Science & Applications* 11, no. 1 (2022): 319.

278. E. Nehme, D. Freedman, R. Gordon, et al., "DeepSTORM3D: Dense 3D Localization Microscopy and PSF Design by Deep Learning," *Nature Methods* 17, no. 7 (2020): 734–740.

279. W. Ouyang, A. Aristov, M. Lelek, X. Hao, and C. Zimmer, "Deep Learning Massively Accelerates Super-Resolution Localization Microscopy," *Nature Biotechnology* 36, no. 5 (2018): 460–468.

280. Y. Zhang, Y. Xie, W. Liu, et al., "DeepPhagy: A Deep Learning Framework for Quantitatively Measuring Autophagy Activity in *Saccharomyces cerevisiae*," *Autophagy* 16, no. 4 (2019): 626–640.

281. D. Morone, A. Marazza, T. J. Bergmann, and M. Molinari, "Deep Learning Approach for Quantification of Organelles and Misfolded Polypeptide Delivery Within Degradative Compartments," *Molecular Biology of the Cell* 31, no. 14 (2020): 1512–1524.

282. I. Belevich and E. Jokitalo, "DeepMIB: User-Friendly and Open-Source Software for Training of Deep Learning Network for Biological

16000854, 2024, 10, Downloaded from https://onlinelibrary.wiley.com/doi/10.1111/tra.12957 by Biblioteca universitaria di Lugano, Wiley Online Library on [18/11/2024]. See the Terms and Conditions (https://onlinelibrary.wiley.com/terms-and-conditions) on Wiley Online Library for rules of use; OA articles are governed by the applicable Creative Commons License

Image Segmentation," *PLoS Computational Biology* 17, no. 3 (2021): e1008374.

283. L. Von Chamier, R. F. Laine, J. Jukkala, et al., "Democratising Deep Learning for Microscopy With ZeroCostDL4Mic," *Nature Communications* 12, no. 1 (2021): 2276.

284. E. Gómez-De-Mariscal, C. García-López-De-Haro, W. Ouyang, et al., "DeepImageJ: A User-Friendly Environment to Run Deep Learning Models in ImageJ," *Nature Methods* 18, no. 10 (2021): 1192–1195.

285. R. Seifert, S. M. Markert, S. Britz, et al., "DeepCLEM: Automated Registration for Correlative Light and Electron Microscopy Using Deep Learning," *F1000Research* 9 (2020): 1275.

286. J. J. Klein, N. C. Baker, K. M. Zorn, et al., "Data Mining and Machine Learning for Lysosomal Disease Drug Discovery and Beyond," *Molecular Genetics and Metabolism* 126, no. 2 (2019): S86.

287. L. Montava-Garriga, F. Singh, G. Ball, and I. G. Ganley, "Semi-Automated Quantitation of Mitophagy in Cells and Tissues," *Mechanisms of Ageing and Development* 185 (2020): 111196.

288. W. Ouyang, F. Beuttenmueller, E. Gómez-De-Mariscal, et al., "BioImage Model Zoo: A Community-Driven Resource for Accessible Deep Learning in BioImage Analysis," *bioRxiv* (2022): 1–28.

289. S. M. Towhidul Islam Tonmoy SMMZ, V. Jain, A. Rani, V. Rawte, A. Chadha, and A. Das, "A Comprehensive Survey of Hallucination Mitigation Techniques in Large Language Models," arXiv:2401.01313, 2024.

290. A. Zou, Z. Wang, N. Carlini, J. M. Nasr, Z. Kolter, and M. Fredrikson, "Universal and Transferable Adversarial Attacks on Aligned Language Models," arXiv:2307.15043, 2023.

291. M. Ranjbar, J. J. Yang, P. Kumar, D. R. Byrd, E. L. Bearer, and T. I. Oprea, "Autophagy Dark Genes: Can We Find Them With Machine Learning?," *Natural Science* 3, no. 3 (2023): e20220067.

292. J. Wu, S. Liu, X. Chen, H. Xu, and Y. Tang, "Machine Learning Identifies Two Autophagy-Related Genes as Markers of Recurrence in Colorectal Cancer," *Journal of International Medical Research* 48, no. 10 (2020): 030006052095880.

293. R. Krueger, J. Beyer, W.-D. Jang, et al., "Facetto: Combining Unsupervised and Supervised Learning for Hierarchical Phenotype Analysis in Multi-Channel Image Data," *IEEE Transactions on Visualization and Computer Graphics* 26, no. 1 (2020): 227–237.

294. W. A. Omta, R. G. Van Heesbeen, I. Shen, et al., "Combining Supervised and Unsupervised Machine Learning Methods for Phenotypic Functional Genomics Screening," *SLAS Discovery* 25, no. 6 (2020): 655–664.

295. F. Maturo and R. Verde, "Combining Unsupervised and Supervised Learning Techniques for Enhancing the Performance of Functional Data Classifiers," *Computational Statistics* 39, no. 1 (2024): 239–270.

296. V. Liss, B. Barlag, M. Nietschke, and M. Hensel, "Self-Labelling Enzymes as Universal Tags for Fluorescence Microscopy, Super-Resolution Microscopy and Electron Microscopy," *Scientific Reports* 5 (2015): 17740.

16000854, 2024, 10, Downloaded from https://onlinelibrary.wiley.com/doi/10.1111/tra.12957 by Biblioteca universitaria di Lugano, Wiley Online Library on [18/11/2024]. See the Terms and Conditions (https://onlinelibrary.wiley.com/terms-and-conditions) on Wiley Online Library for rules of use; OA articles are governed by the applicable Creative Commons License